TITLE

Manufacturing, characteristics and applications of auxetic foams: A state-of-the-art review

AUTHORS

Jiang, W; Ren, X; Wang, SL; et al.

JOURNAL

Composites Part B: Engineering

DEPOSITED IN ORE

23 February 2022

Manufacturing, characteristics and applications of auxetic foams: A state-of-the-art review

Wei Jiang[a], Xin Ren[a, *], Shi Long Wang[a], Xue Gang Zhang[a], Xiang Yu Zhang[a], Chen Luo[a], Yi Min Xie[b], Fabrizio Scarpa[c], Andrew Alderson[d], Ken E. Evans[e]

[a] *College of Civil Engineering, Nanjing Tech University, Nanjing, Jiangsu, 211816, PR China*

[b] *Centre for Innovative Structures and Materials, School of Engineering, RMIT University, Melbourne, 3001, Australia*

[c] *Bristol Composites Institute, University of Bristol, BS8 1TR Bristol, United Kingdom*

[d] *Materials and Engineering Research Institute, Sheffield Hallam University, Sheffield, United Kingdom*

[e] *College of Engineering, Mathematics and Physical Sciences, University of Exeter, EX4 4QF Exeter, United Kingdom*

* Corresponding author: Xin Ren. Email: xin.ren@njtech.edu.cn

Abstract:

Auxetic foams counter-intuitively expand (shrink) under stretching (compression). These foams can exhibit superior mechanical properties such as resistance to shear and indentation, improved toughness and energy absorption (EA) under several types of loadings. Their unique deformation mechanism and manufacturing process lead to special multiphysics properties such as variable permeability, synclastic curvature and shape memory. Except for traditional energy absorber stuff, the potential applications of auxetic foams have involved biomedicine, aerospace, smart sensing, etc. However, most of the potential applications are restrained in the theoretical stage due to complicated fabrication and a deficiency of stability. For removing the barrier for practical application, a series of issues remain to be resolved, though the explorations of the improved conversion methodologies and potential applications are fruitful in the past decades. We present here a review article discussing the state-of-the-art for manufacturing, characterization and applications of auxetic foams. We also provide a view of the existing challenges and possible future research directions, aiming to state the perspective and inspire researchers to further develop the field of auxetic foams.

Keywords: auxetic, foam materials, smart materials, negative Poisson's ratio, protection equipment

1. Introduction

The Poisson's ratio (denoted ν for isotropic materials) is a parameter that defines the ratio between the lateral deformation of a body subjected to axial loading, i.e., between the transverse strain (ε_t) and the longitudinal strain (ε_l) with the minus sign ($-\varepsilon_t/\varepsilon_l$ [1]). According to the classical theory of elasticity, the Poisson's ratio for isotropic materials ranges from - 1 to 0.5 [2], so that a negative Poisson's ratio is allowable in linear elastic and thermodynamically correct materials. Most of normal materials become fat (thin) under compression (tension), and so exhibit a positive Poisson's ratio behaviour. In contrast, negative Poisson's ratio materials show a counter-intuitive behaviour under axial loading - they become thin (fat) under compression (tension) (**Figure. 1**).

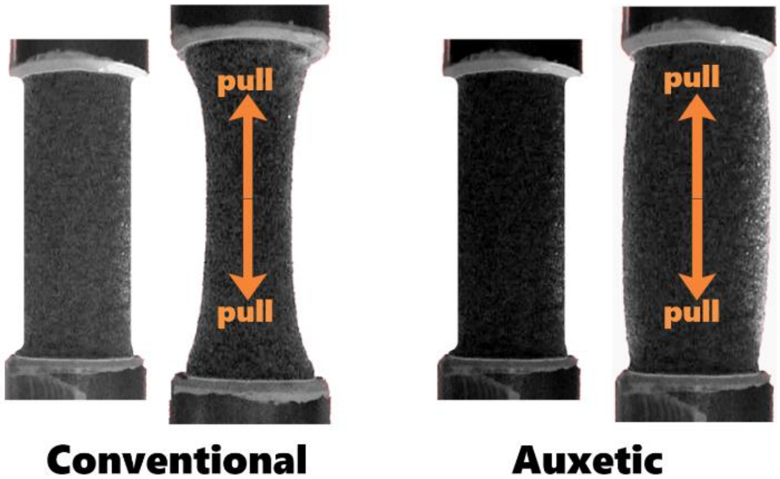

Figure. 1. Shape changes under stretching of conventional foams (left) and auxetic foams (right).

The term "auxetic" was introduced by Evans [3] who adapted the ancient Greek word "auxetos" (that which tends to increase) for negative Poisson's ratio materials. Iron pyrite monocrystals was reported as possessing an auxetic behavior since 1882 [2], with a Poisson's ratio value of - 1/7 estimated by Love [4]. Natural auxetic materials that have been reported in open literature also include cow teat skin [5], cat skin [6], cancellous bone [7] and membranes found in the cytoskeleton of red blood cells [8]. Wojciechowski [9] also demonstrated the existence of negative Poisson's ratio in cyclic hexamers molecule assemblies subjected to critical pressure levels.

Foam materials possess many superior properties, such as improved performance under the impact, lightweight, cost-effective, reusable, desirable acoustic capability, and remarkable chemical and physical stability [10-14]. In this context, foam material has been widely used in daily life and is considered a potential candidate for multifunctional engineering materials. On the other hand, foam materials have high resilience and can bear large strain deformation. Such properties are desirable to auxetic materials which need enough axial deformation for the showing of unique lateral deformation. Therefore, it could be expected that foam material would exhibit more remarkable and functional properties if it be endowed with auxetic performance.

The first artificial auxetic open cell foam fabricated using a combination of volumetric compression and thermoforming was reported by Lakes in 1987 [15]. During the following decades, increasing numbers of artificial auxetic materials have been developed at different scales [16] (**Figure. 2**) and one typical methodology, pattern scale factor (PSF) methodology was proposed to artificially design the auxetic unit cells with tunable mechanical performance [17, 18]. A good portion of artificial auxetic materials is fabricated via textiles or 3D printing, whereas auxetic foams can be produced by post-processing existing conventional off-the-shelf porous materials.

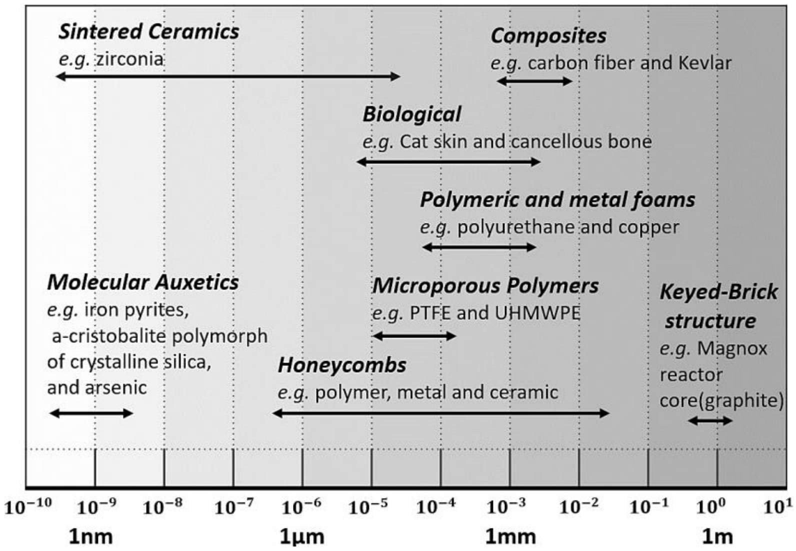

Figure. 2. Categories of auxetics at different scales (Reproduced from [19]).

Though several reviews on auxetic materials have been published in the past decades [16, 19-28], a more focused review on auxetic foams is still rare. Considerable progress in the fabrication, characterization and applications of auxetic foams has been reported in the past eight years since the publication of last review on auxetic foams [29]. In this paper, state-of-the-art review and the problems accompanied with possible solutions of current researches on the manufacture, characteristics and applications of auxetic foams have been made, aiming to inspire the peers and pave the way for further studies (**Figure. 3**).

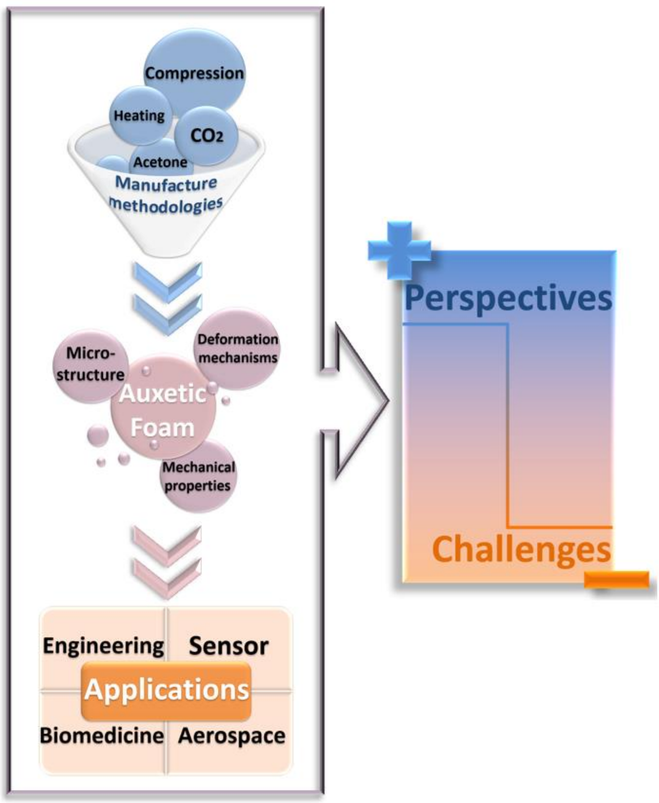

Figure. 3. Outline of this article.

2. Manufacture methodologies for auxetic foams

The principle for transforming traditional foams into auxetic form consists in producing a stable compression that induces the lattice into a re-entrant shape. The volumetric compression can be generated either by mechanical or via air pressure at first, and the foams ribs can then be softened into shape by applying a specific heating profile or chemical solvent, followed by the re-entrant shape fixed by the annealing and a cooling stage. Softening and cooling are however unnecessary for metal foams (copper foam) (**Figure. 4**) [30-33] due to the high plasticity and the possibility of creating the re-entrant shape by plastic deformations only. Methodologies for the conversion of auxetic foams are fruitful and still on-going, current foam materials that can be converted into auxetics are listed in **Table. 1**.

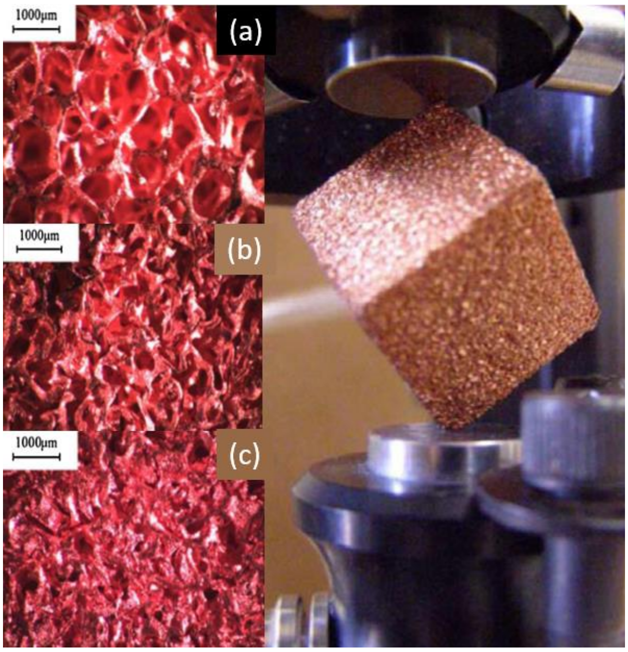

Figure. 4. Microstructures of copper foam subjected to volumetric compression ratios (VCR: Initial / Final Volume) of (a) 1, (b) 4.43 and (c) 4.94 respectively (Adapted from [33]).

Table. 1. Examples of several foam samples that have been managed to be converted into auxetics ("ppi" means "pores per inch" - the most common unit for foam pore size).

material		pore diameter (mm)	density (kg/m³)	reference
polyester urethane foam	closed-cell	0.42 (60 ppi)	37.9	[37]
	reticulated	0.42 (60 ppi)	33.7	[37]
	open-cell	2.54 (10 ppi)	24.1	[37]
		0.85 (30 ppi)	24.5	
		0.42 (60 ppi)	21.7	
open-cell polyurethane foam		2.54 (10 ppi)	34	[70]
		1.27 (20 ppi)	30	[66]
		0.73-0.85 (30-35 ppi)	32	[113]
		0.73-0.85 (30-35 ppi)	27	[144]
		0.56 (45 ppi)	27	[70]
		0.45-0.49 (52-57 ppi)	27	[38]
		0.39 (65 ppi)	30	[66]
		0.25 (100 ppi)	30	[66]
closed-cell polyethylene foam		20 (expansion ratio)	not given	[53]
		30 (expansion ratio)	not given	
		45 (expansion ratio)	not given	
closed-cell polyvinyl chloride (PVC) foam		not given	52	[53]
open-cell copper foam		1	not given	[30]
room temperature vulcanizing elastomeric silicone foam		not given	150	[30]
closed-cell polymethacrylimide foam		not given	52	[44]
			205	
			301	
closed-cell polyethylene foam		not given	59	[44]
			109	
			158	

2.1 Original and improved thermo-mechanical methodologies

In 1987, the first auxetic foam with Poisson's ratio value of - 0.7 was converted from conventional commercial open-cell polyurethane (PU) foam by Lakes [15] through a thermo-mechanical (mechanical compression and thermoforming) methodology (**Figure. 5a**). Samples of conventional foam were compressed along three orthogonal directions and placed in a mold at a temperature slightly higher than the softening one of the foam samples (163°C to 171°C). The mold was then cooled and the resulting foam showed stable buckled ribs and negative Poisson's ratio. Uniaxial compression was also applied but could only enable the production of foams with a near zero Poisson's ratio rather than a negative value [15]. However, further studies have shown that foam samples that are sufficiently thin could provide a negative but inhomogeneous distributed Poisson's ratio under only uniaxial compression [34, 35].

The thermo-mechanical methodology could also convert polyvinyl chloride (PVC) foams [36, 37], closed-cell PU [38] and silicone rubber foam [30] into auxetic foam. As for metal foam (copper foam), the heating stage is however not necessary because the conversion could happen under sequential plastic compression along three directions [30-33]. Friis *et al.* [30] produced auxetic PU foam by applying triaxial compression during the foaming process without the heating phase as well.

The toughest manufacturing limitations of the thermo-mechanical methodology are, especially in manufacturing large foam samples, the sufficiency of long-term stability in mechanical properties, risk of creasing surface and uneven heating and / or compression during manufacturing. To overcome these drawbacks, several improvements based on the thermo-mechanical methodology have been introduced (**Figure. 5**). A quasi tri-axial methodology (**Figure. 5b**) was described by Mohsenizadeh *et al.* [39]. A novel mold was introduced to split the compression process into three stages (x-compression, y-compression and z-compression), ensuring that foam samples are evenly compressed in three directions. Foam samples fabricated using this methodology showed a better homogeneity, rigidity and isotropic behaviour and effectively overcame the surface creasing problem. Duncan *et al.* [40] developed a novel cuboidal mold with through-thickness pins (**Figure. 5c**) to reduce folds on the foam surface and improve the uniformity of compression throughout the sample. The use of pins to control the internal compression state of the foam, in addition to the external compression applied by the mold, was first introduced by Sanami *et al.* in the production of one-piece radially gradient "core-sheath" foams having distinctly different core and sheath region pore structures, Poisson's ratios (including negative), and Young's moduli [41]. Subsequentially, Duncan *et al.* [42] designed a novel mold with partly distributed through-thickness pins for fabricating gradient auxetic foam sheets. This mold was partitioned to generate different fabrication and compression processes, which could significantly shorten the manufacturing time of different types of foam samples. The work of Duncan *et al*. also highlighted the advantages brought by through-thickness pins approach. Except for introducing novel molds to improve compression quality, some additional processes are also effective to obtain auxetic foam samples with better performance in stability and mechanical properties. Chan *et al.* [38] proposed a multi-stage process enabling conventional foam samples to be converted twice in different VCR (**Figure. 5d**) for a gradual compression. This process can effectively avoid the creasing of the surfaces that occurs during original one-stage compression and exhibits the potential benefit to manufacture large foam samples. Bianchi [43, 44] applied a re-heating process (**Figure. 5e**) on the samples recovered from auxetic foams. The stability of the auxeticity and the mechanical properties of the auxetic foam samples could be significantly enhanced by re-manufacturing.

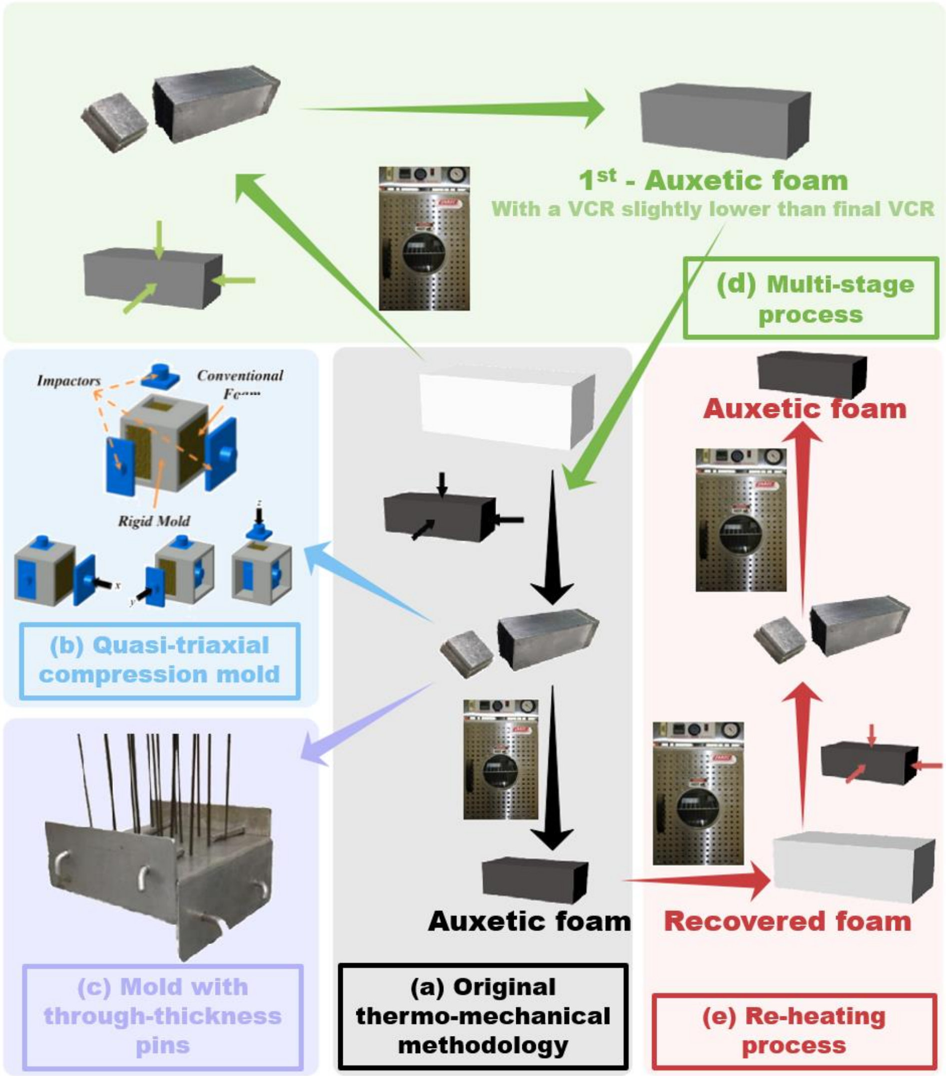

Figure. 5. Current methodologies based on the thermo-mechanical methodology of (a) original thermo-mechanical methodology [15], introducing of (b) quasi tri-axial mold [39] and (c) cuboidal mold with through-thickness pins [40] for uniform compression, (d) adopting a pre-auxetic process to realize multi-stage (gradual) compression [38], and (e) a double thermo-mechanical process to convert the recovered foam to obtain twice-processed auxetic foam samples with long-term shape stability [43, 44].

Two alternative compression techniques to produce the volumetric compression have been also elsewhere developed. The early study of Martz *et al.* [45] reported that closed-cell polymethacrylimide (PMI) and low-density polyethylene (LDPE) foams could show an auxetic behaviour under high external air pressure followed by heating process. Air pressure (or suction) was also used in the “half mould” manufacturing process proposed by Bianchi *et al.* [46] to manufacture auxetic foams samples with curved and arbitrary shapes. By using engineered vacuum, Zhang *et al.* [47] fabricated foam samples having a stiffness 5 times larger than the stiffest auxetic foam presented in open literature, meeting the requirements of both high stiffness and auxeticity. Hydro-static pressure has been also applied by Najarian *et al.* [48] as another tool to compress the foam samples.

2.2 Adopting of acetone, CO2, steam penetration and condensation (SPC) and 3D printer

One of the earliest explanations of the auxetic behavior in negative Poisson's ratio foams is based on the "missing rib" concept, i.e., the failure and breaking of ribs during the volumetric compression leading to changes of the original pore cell geometry. Smith *et al.* [49] therefore predicted that foam ribs might be removed following a chemical process so the foam samples could turn into auxetics. In 2009, Grima [50] realized the predicted conversion of auxetic foams by placing compressed foam samples within a container in acetone to soften foam ribs, rather than applying a temperature profile for the annealing. Inspired by this novel softening process, an improved chemo-mechanical methodology (the Mechanic-Chemic-Thermal technique) (**Figure. 6**) was then developed by the Air Force Institute of Technology (AFIT) in Poland [51]. Compared with foams fabricated using the original thermo-mechanical methodology [52], auxetic foams softened by chemical process could obtain a lower Poisson's ratio without the risk of uneven heating, and this approach is potential to produce large samples, however in considering of the safety hazard and environmental footprint issues, such chemical softening process is not recommended in further researches.

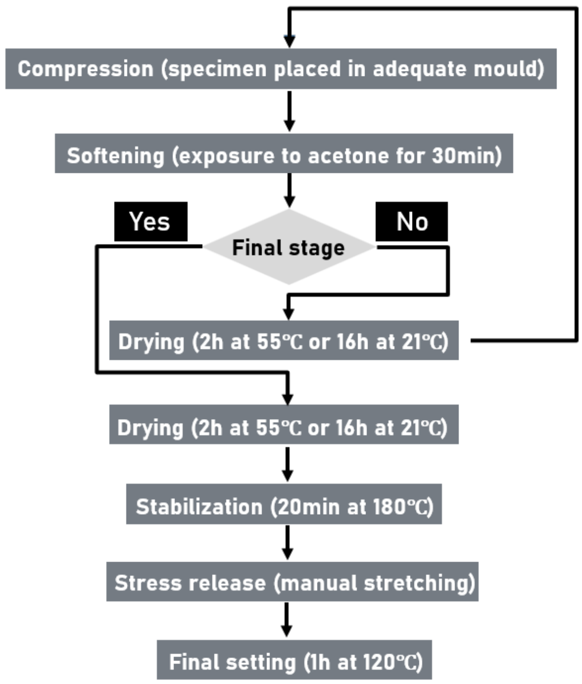

Figure. 6. Flow chart depicting the four stages auxetic foam manufacturing process proposed by AFIT (Adapted from [51]).

For developing a more environment-friendly fabrication process, Li [53] adopted CO_2 as the main softening agent. Carbon dioxide could reduce the glass transition temperature of Styrene acrylonitrile copolymer (SAN) particles (copolymers in PU foams, play the key role in foam ribs softening) after a series of chemical reactions. Auxetic foams treated with carbon dioxide could be rapidly converted at a room temperature and exhibited a nearly constant value of negative Poisson's ratio over a large strain range. Recently, basing on the function of CO_2 in the manufacturing, high-performance closed-cell auxetic nylon elastomer (NE) foams with Poisson's ratio value of - 1.29 and superior mechanical properties have been fabricated by Fan *et al.* [54] using a green and environment-friendly methodology named One-Pot CO_2 foaming process (**Figure. 7a**). Fan *et al.* have also remarked that this methodology could be also applied to other polymers (like ethylene-vinyl acetate (EVA） resins). SPC methodology (**Figure. 7b**) was described by Fan *et al.* [36], which enabled the development of auxetic closed-cell polyethylene (PE) and PVC foams. This methodology could also be used for fabricating large auxetic foam samples as a related paper of Duncan *et al.* [55] shows.

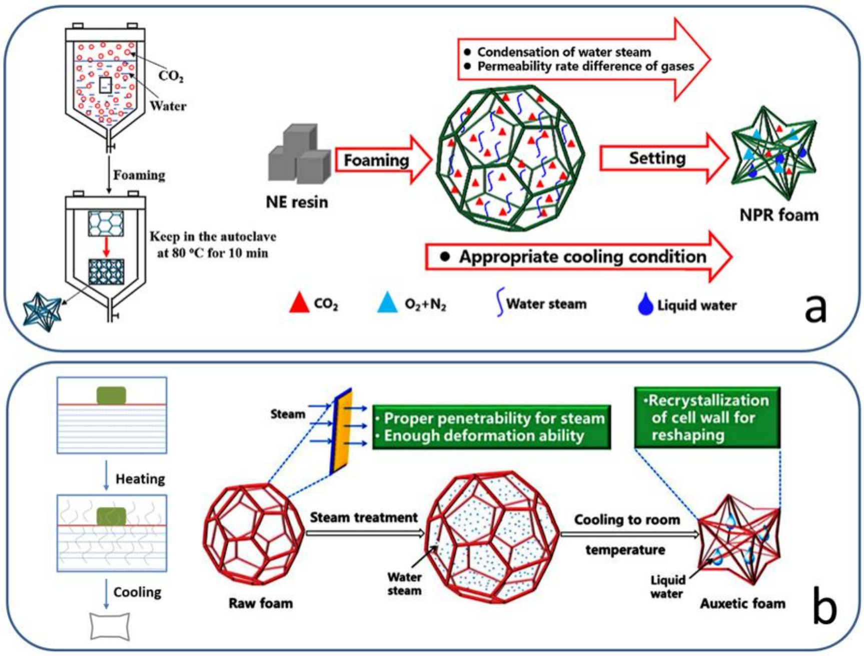

Figure. 7. Schematic drawings showing the experimental flow chart (left) and possible formation mechanism (right) of a) One-Pot CO_2 foaming process and b) SPC process (Adapted from [54] and [36]).

With the rapid development of 3D print technology, complicated 3D structures can be fabricated with increasingly high precision in 3D printers. Except for traditional methodologies to convert foam materials into auxetics, a novel concept of manufacturing auxetic foams by 3D print technology was proposed by Critchley *et al.* [56], the foam samples they manufactured were customized designed and fabricated without any random cell orientation, providing a new methodology to generate foam structures with stability and homogeneity (**Figure. 8**). However, relatively high costs, scale limitation and the presence of defects still impede the broad application of this technique. From this perspective, the rest of porous auxetic structures fabricated by 3D printers could be defined as a novel foam material in a broad sense (Syntactic foams [28, 57-65]). Such structures are potential alternatives as polymer foam materials to some applications such as sensors or soft robots, providing stable and precise reactions under loadings.

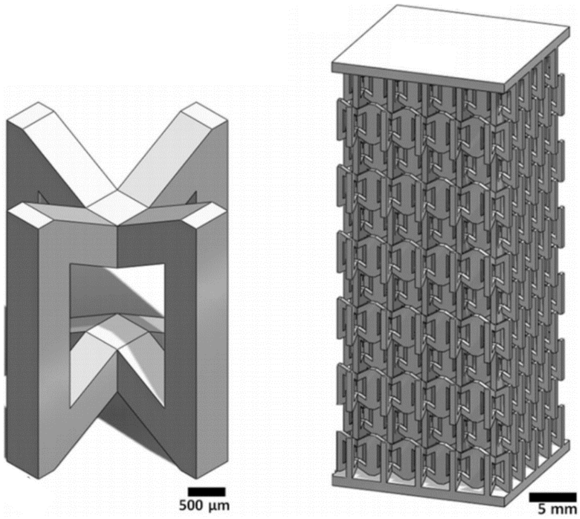

Figure. 8. The unit cell (left) and the whole model (right) of auxetic foam fabricated by 3D print technology [56].

Although the methodologies mentioned above are feasible to convert conventional foams into auxetics, most of them are restricted in a small dimension. Large samples cannot be compressed and softened in an even manner, resulting in sometimes substandard performance. Many potential applications for which auxetic foams could be extremely advantageous to use (cushions and pads, for example) are still confined at the stage of design and prototyping, waiting for low-cost and efficient large scale manufacturing routes to be fully developed.

2.3 Parametric manufacturing

Several research teams have looked at identifying the most important manufacturing parameters that improve the quality and performance of auxetic foams. In relation to the thermo-mechanical methodology, the debate about the best combinations of those parameters (temperature, heating time and VCR) has started since the beginning of the original productions of auxetic foams. The first negative Poisson's ratio polymer foam fabricated by Lakes [15] was subjected to VCR values from 1.4 to 4 and heating temperatures between 163°C and 171°C, heating time was however unmentioned in his work. Friis *et al.* [30] indicated that 200°C may be a more suitable temperature to soften the foam ribs for the tested PU foams of solid volume fraction 0.043. The heating time and VCR adopted in the work are 7 min and 3.4, respectively. Wang *et al.* treated 40 100 ppi (pore diameter of 0.25 mm) PU foam specimens (the density was 0.033 g/cm^3) under different combinations of manufacturing parameter to investigate the influence of the temperature and heating time on the final value of the Poisson's ratio [66] (**Figure. 9**). In the work of Choi *et al.* [67], two types of open-cell PU foams (gray polyurethane-polyester foam: $\rho/\rho_s = 0.03 \pm 10\%$, L (length of cell rib) = 0.4 ± 0.03 mm and Scott industrial foam: $\rho/\rho_s = 0.03 \pm 7\%$, L = 1.2 ± 0.03 mm) have been produced by using different parametrical combinations. The lowest value of the Poisson's ratio achieved in that work was - 0.7, for both kinds of foam, obtained from a VCR between 3.3 to 3.7 under a heating temperature of 170 °C for 17 min. Moreover, another paper of Choi' group shows that the VCR should be smaller than 5 to avoid contact between ribs and adhesion [67].

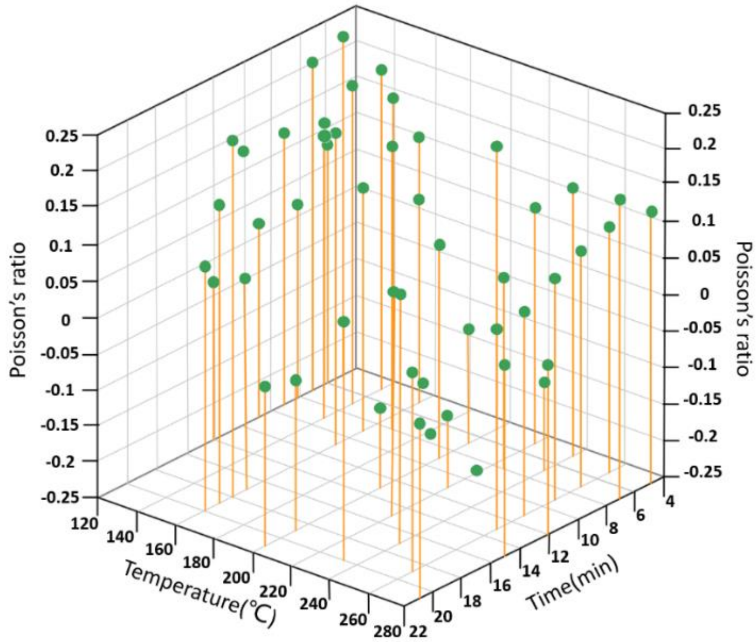

Figure. 9. Poisson's ratio of auxetic foams fabricated from 100 ppi (pore diameter of 0.25 mm) PU foams with VCR of 2.5 and different combinations of temperature and heating time (Data replotted from [66]).

Martz *et al.* [45] noted that excessive temperature exposure (220 °C) could only make transformed PMI closed-cell foams stiffer without auxeticity, the reason for this phenomenon may be the adhesion of melted foam walls. Duncan *et al.* [68] reported that a temperature higher than 200 °C would however induce a substantial mass loss of the open-cell PUR30FR foams, and a combination of high temperature and long heating times could only make them exhibit auxeticity in tension. The optimal parametrical combination they provided are VCR = 3, 130 °C, 140 °C, and 160 °C for 180, 60, and 20 min, respectively, resulting in a minimum ν = - 0.2. As for heating time, Chan and Evans [38] proposed that foam samples could not be "set" and were apt to recover to their original shape (or be melted into a block of dense material) if the heating time was too short (or too long in the case of melting). The critical temperatures of reticulated PU foams in three phases (softening around 180 °C, liquefaction around 270 °C and polymer decomposition around 300 °C) were also noted in the paper. Temperatures about 5 - 20 °C lower than the softening temperature were suggested advisable to maximize the stress relaxation and minimize the possible bonding between cell ribs. Wang and Lakes [66] then proposed a series of optimal combinations of temperature and heating times for open-cell PU foam samples with different cell sizes (25 ppi, 65 ppi and 100 ppi, i.e., pore diameter of 1 mm, 0.39 mm and 0.25 mm, respectively). All samples were produced with the same VCR of 2.5. Detailed parameters and results are presented in **Figure. 10**. The first design of experiment (DoE) work related to the manufacturing of open cell PU auxetic foams was carried out by Bianchi *et al.* [69]. The Authors of that work carried a systematic campaign of quasi-static cyclic tension/compression tests on 80 different cylindrical foam specimens with

VCRs ranging between 5 and 19, two temperatures (135 °C and 150 °C), two heating times (12 min and 15 min) and also two different cooling methodologies (water and air ventilation). The final conclusions of the DoE showed that the VCR is the most statistically important manufacturing, while no significant statistical correlation could be identified with the temperature, heating times provided and the cooling methodologies. Critchley *et al.* [70] recently provided an updated statistical approach for the optimization of the manufacturing parameters to improve the efficiency of the production. An optimal combination of VCR, porosity and heating time was recommended for a conversion temperature of 200 °C, detailed parameters are also shown in **Figure. 10**. In view of practical applications, especially for applications in EA, the final density is however indicated as a critical parameter [69, 71, 72]. A lower VCR appears to be preferable to maximize EA under quasi-static compression [73]. A VCR value of 2.2 was recommended as the best for PU foams used in seat cushions [71].

To determine the effect of the material plasticity on energy dissipation of auxetic metal foams, numerical impact tests on foam finite element (FE) models have been carried out by Kumar *et al.* [74]. The plastic Poisson's ratio (the Poisson's ratio on the plastic stage v_p should be close to zero to obtain the maximum energy dissipation.

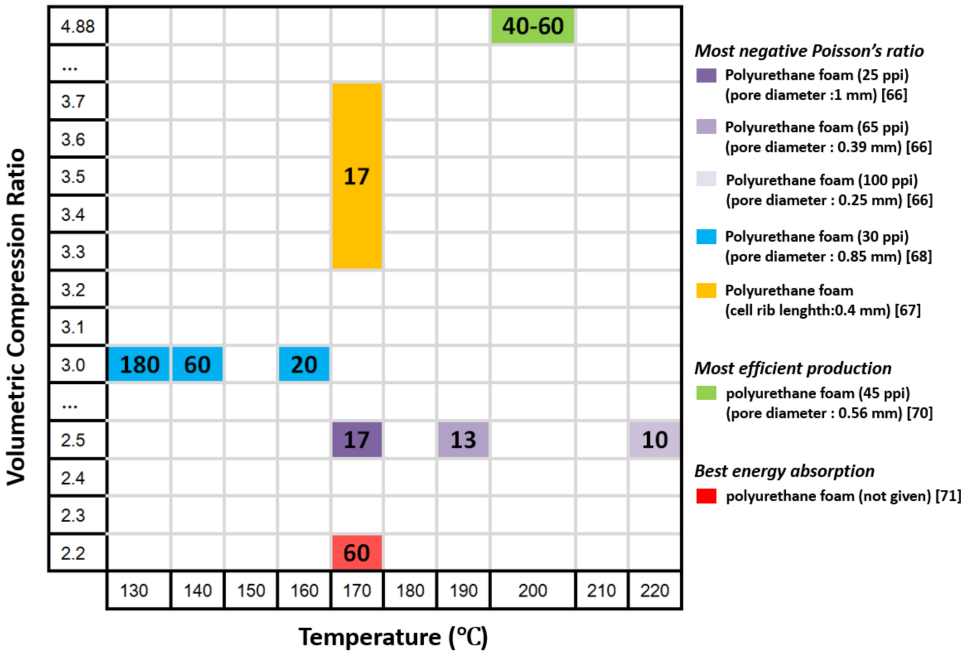

Figure. 10. Summary of the recommended parametric combinations based on experiments in the literature of heating temperature, VCR and heating time (indicated by the number in blocks, measured in minutes) for different foam samples (indicated by the color of blocks) (Data obtained from [66-68, 70, 71]).

PU foam samples were compressed using hydro-static pressure before being placed into the mold in the work of Najarian *et al.* [48], so the value of the pressure is also a critical parameter during in the conversion process in the work. In order to obtain foam samples with the best auxeticity and stiffness, a grey relational analysis (GRA) was proposed in the paper to control the influential parameters *viz.* temperature, pressure and time. The optimal combination of parameters involved the values of 140 °C for the annealing temperature, 40 bar for pressure and 20 min for heating time. Duncan *et al.* [55] recently investigated the effect of steam conversion on the cellular structure, Young's modulus and negative Poisson's ratio of closed-cell LDPE foams. The formation of cells with re-entrant shape tended to increase with the duration of steam conversion. Surprisingly, large foam samples in the fabrication shrank more evenly than small ones, indicating this methodology is a feasible way to fabricate large foam specimens.

Though lots of investigations have been conducted and the conclusions include detailed parametric combinations to manufacture optimal auxetic foams, the recommended combinations are regarded as reference to further experiments due to the variation of foam samples (such as chemical constituents and sample size) and randomness of manufacturing condition (such as room temperature for cooling). The size of foam samples, in fact, is of significance in the manufacturing consisting in heating process and should be taken into further consideration.

3. Micro-structure and deformation mechanisms in auxetic foams

Solid understanding of micro-structure and deformation mechanism in auxetic foams is not only the foundation to explore efficient manufacturing methodologies, but also desirable to create valid foam models using in numerical analysis and finite element modeling (FEA). Such models could also be utilized for inspiring auxetic structural design.

3.1 Re-entrant polyhedron models of auxetic foams

The first step in developing micromechanical models for these foams is to define the geometry of the original and converted foam cells. The internal pressure and squeezing of neighbor cells or surfaces during the foaming stage generate cells with multiple polyhedron shapes. Most of the earliest studies on foam structures have been focused on simplified topological representations involving faceted polyhedrons (**Figure. 11**). Lakes [15] is the first to present stereo photographs and an idealized re-entrant unit cell structure for the auxetic foams, in which the ribs were bent and protruded into the cells: an axial tensile load would cause the cell to unfold and expand laterally. Later, Friis [30] developed the topology of the model further by using the Kelvin minimum area tetrakaidecahedron consisting in a convex shape with eight curved hexagonal faces and six curved square faces. However, the description of how conventional foam deforms was absent. Wei [75] extended the lattice formulation of Warren and Kraynik [76] to represent polymeric networks via three arms of equal length and one backbone all connected to one junction. The model could be applied to both 2D and 3D cases. Choi *et al.* [77] proposed a novel 3D tetrakaidecahedron model companied by a description of how it could assume a re-entrant structure. Doyoyo *et al.* [78] presented a 3D auxetic structural lattice and verified that it could predict some mechanical properties of previously published auxetic foam materials. Cham et al. [79] argued that the tetrakaidecahedron model is not adequate to consider anisotropic foams with a preferential rise direction during foaming or thermoforming, and therefore introduced a more generally accepted dodecahedron model.

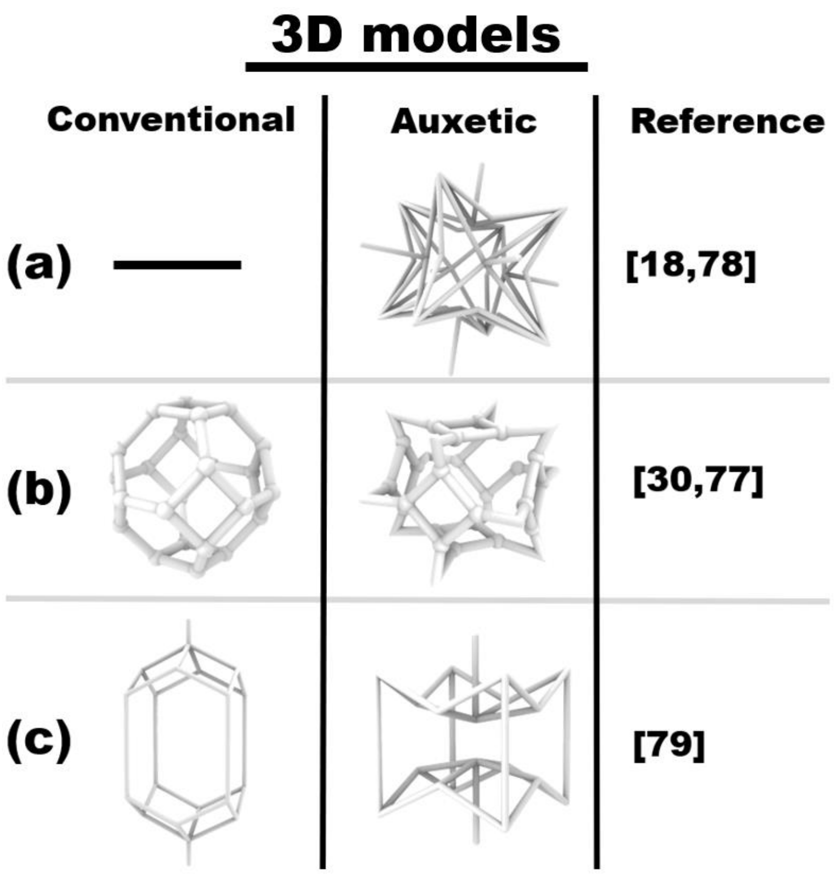

Figure. 11. 3D polyhedral models of auxetic foams proposed in literature: (a) Idealized re-entrant unit cell structure, original foam structure is not given in the paper [18,78], (b) Kelvin minimum area tetrakaidecahedron model [30,77] and (c) Dodecahedron model [79].

3.2 2D models of auxetic foams

Various 2D models have also been developed to provide a more simple explanation of potential deformation mechanisms occurring inside auxetic foams when subjected to loading (**Figure. 12**). The 2D lattices derived from 3D configurations could be also helpful to inspire the design of general 2D auxetic materials. Early studies considered the auxetic structure of the foam as derived from the hexagonal configuration lattice [42, 80, 81] and modified those centrosymmetric topologies into auxetic ones [42, 80-83]. In those models the auxetic behaviour requires the deformation of the foam ribs from "Y" shape to "arrow-head" joints (i.e., the re-entrant structure). Another 2D model named "missing rib"model was proposed by Smith *et al.* [49]. This model could explain the auxeticity and the strain-dependent Poisson's ratio behaviour by further fitting some of its parameters to experimental data. Further modifications of the missing rib model were introduced by Gaspar *et al.* [84] and Lim *et al.* [85], with improved accuracy in terms of the prediction of the Poisson's ratio of the auxetic foams. However, Gaspar *et al.* [86] also noted that missing ribs are actually existing in real auxetic foams, but their fraction over the total of the foam ribs is quite small and the dominant deformation within the auxetic cells is still the bending of straight ribs.

In 2005, Grima [87] proposed a system based on rotating components linked by rigid or flexible joints / ribs to explain the deformation mechanism in auxetic foams when compressed. The rigid joints inside the foams could be simplified into triangles [87-89] . Pozniak *et al.* [90] have developed two 2D models of auxetic foams (Y and △ models). These two simple disordered structures could predict well the deformation of foams under compression. An extended model was proposed by Chetcuti *et al.* [89] that took into account the amount of material at the joints and the deformation of the joints themselves, this model allowed a set of more plausible predictions of the Poisson's ratio values. Similar disordered structure for simulating auxetic foams is the 2D random cellular solid model proposed by Li *et al.* [91]. Regular 2D Voronoi model was given a irregularity of 0.45 and then modified by a process of merging and removing to correspond with the geometric shape of experimental auxetic foams. Alderson *et al.* [92] proposed three 2D topologies based on the observation of micrographs of auxetic foams to illustrate the effects of uni-axial, bi-axial and tri-axial compression on the pore structure. Simular works have been carried out by Bianchi *et al.* [46] for invastigating the deformation mechanism of converted foam samples fabricated by "half mould" process.

Similarly to 3D models, the 2D models of auxetic foams allow to predict the auxeticity and the mechanical of the porous materials. The deformation mechanisms predicted by these models could also inspire future works in designing novel auxetic structures.

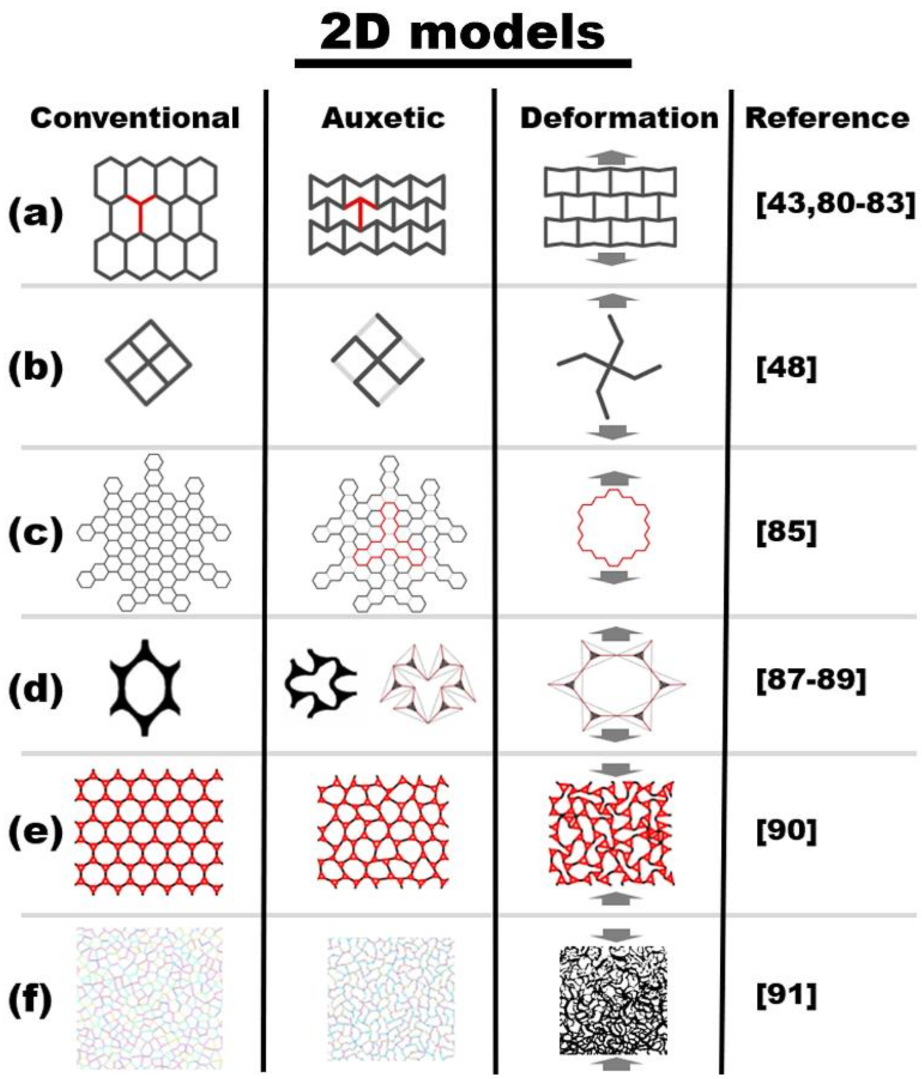

Figure. 12. 2D models of auxetic foams proposed in literature: (a) the transformation of "Y" shape joints to "arrow head" joints [43,80-83], (b) chiral structure produced by "Missing ribs"(broken ribs caused by compression, melt ribs caused by heating process or removed ribs caused by acetone) [48], (c) modified re-entrant "missing rib" model based on hexagonal foam cells [85], (d) regarding the joints as triangle shape, and the deformation based on the rotating of joints which resulting the re-entrance of foam ribs [87-89], and disordered foam structures based on (e) rotational joints model [90] and f) 2D Voronoi model [91].

3.3 Microphotographs and FE models of auxetic foams

The use of various imaging technologies such as digital image correlation (DIC), X-ray scattering, computed tomographic (CT) and scanning electron microscope (SEM) allows to identify the internal structure and deformation mechanism of auxetic foams (**Figure. 13**). Alderson *et al.* [34] observed that the auxetic behaviour of auxetic thin flat pads fabricated by uni-axial compression was due to a through-the-thickness crumpling of the cells, and evidence for the existence of the equivalent of rotation joints has been provided by X-ray microtomography [93, 94]. SEM has also allowed to observe bending, stretching, hinging and obvious rotations of elements of the foam pores during compression [73], indicating the presence of an heterogeneous deformation during the compression of foams. Similar studies based on CT techniques have been carried out by Elliott *et al.* [95], who also observed the presence of bending and entirely collapsed layers of cells and struts impinging on each other during compression.

SAN particles (mentioned in **2.2**, the utilizing of CO_2) were observed in PU foams by Li *et al.* [96], and this nanoparticle compound provided a likely explanation of the annealing temperature mechanism within the fabrication of the foams. The finding of the consisting of SAN copolymers also promotes further invastigations on auxetic foam manufacturing modyfying.

The imaging technologies mentioned above have also allowed to identify strong local heterogeneities of open-cell PU foams [85, 86, 97, 98] , anisotropic behaviour in closed-cell PU foams [39, 97, 99] and open-cell PU foams [46, 47], difference in distribution of reduction in size of cells in the closed-cell PE foam [36] and defects of the foams fabricated using 3D print [56]. Recently, Pashineet *et al.* [100] interpreted the deformation of auxetic foams as a directed aging process, under which foam samples develop along an expected direction at larger scale like network bonds, rather than at microscopic one.

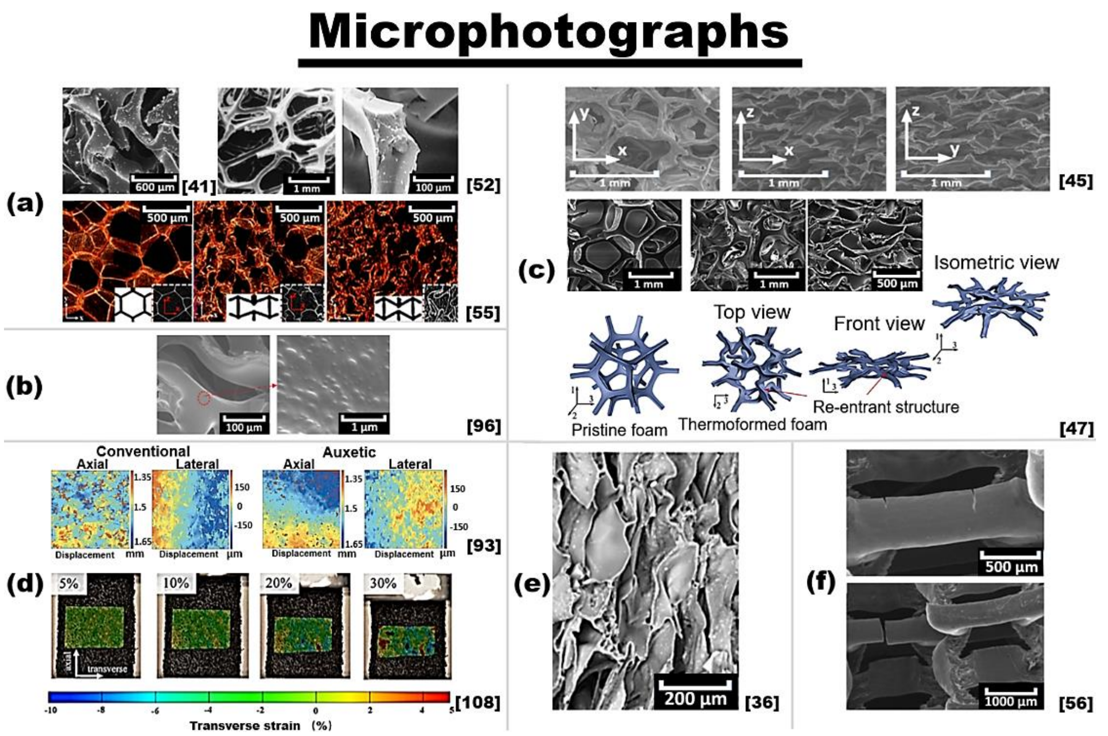

Figure. 13. Images of the microstructure of auxetic foams in literature: (a) Observations of bending, stretching, hinging and obvious rotating during compression [52,55], (b) SAN particles which provided a likely explanation of the annealing temperature mechanism within the fabrication of the foams [96], (c) anisotropic behavior in auxetic foams [45,47], (d) local heterogeneities in auxetic foams [108], (e) difference in shrank distribution in the closed-cell PE foam during the steam treatment [36] and (f) defections of the foams fabricated by 3D print technology [56].

The imaging technologies allow the identification of foam structures and their deformation mechanisms. Micrographs and 3D images obtained by using CT could also be used to develop solid models of the foam skeletons and microstructures, and be transferred to the finite element analysis (FEA) software for simulating the mechanics and deformation mechanisms of these foams at much higher fidelity (**Figure. 14**). Two 3D region of interest models were crated and transformed into FE models by McDonald *et al.* [93]. The local rib interactions and globle dispplacement of foam samples can be faithfully represented by followed FEA process, providing confirmation to the mechanisms observed in the experiments and greater details occurred in foam samples under applied loadings. The above-mentioned 2D auxetic models that proposed by Pozniak *et al.* [90] and Li *et al.* [91] can also be built in FEA softwares. Pozniak *et al.* proposed two approaches for simulating the structures they proposed : the plane stress based and the beam based approach. These two approaches are valid to simulate proposed structures, however, in consideration of both calculation speed and simulating accuracy, the latter approach was recommended as the better one. As for the works of Li *et al.*, different area compression ratios A_r was adopted in structural design to correspond with the different VCRs that adopted in actual copper foams according to ref.[33]. The excellent agreement achieved between FEA and experimental observations shows that these irregular structures can highly simulate the deformation of actual auxetic foam samples. Some mechanical properties such as the Poisson's ratio behavior and EA capacity can also be predicted to some extent by similation results of these structures. In order to investigate the blast resistance of auxetic structures, Li *et al.* [101] built a series of 3D isotropic auxetic foam core in FEA software by using random Voronoi structures. The Poisson's ratio varies from positive to negative by changing the randomness and tri-axial compression ratio of the structures, providing a feasible methodology to build auxetic FE models.

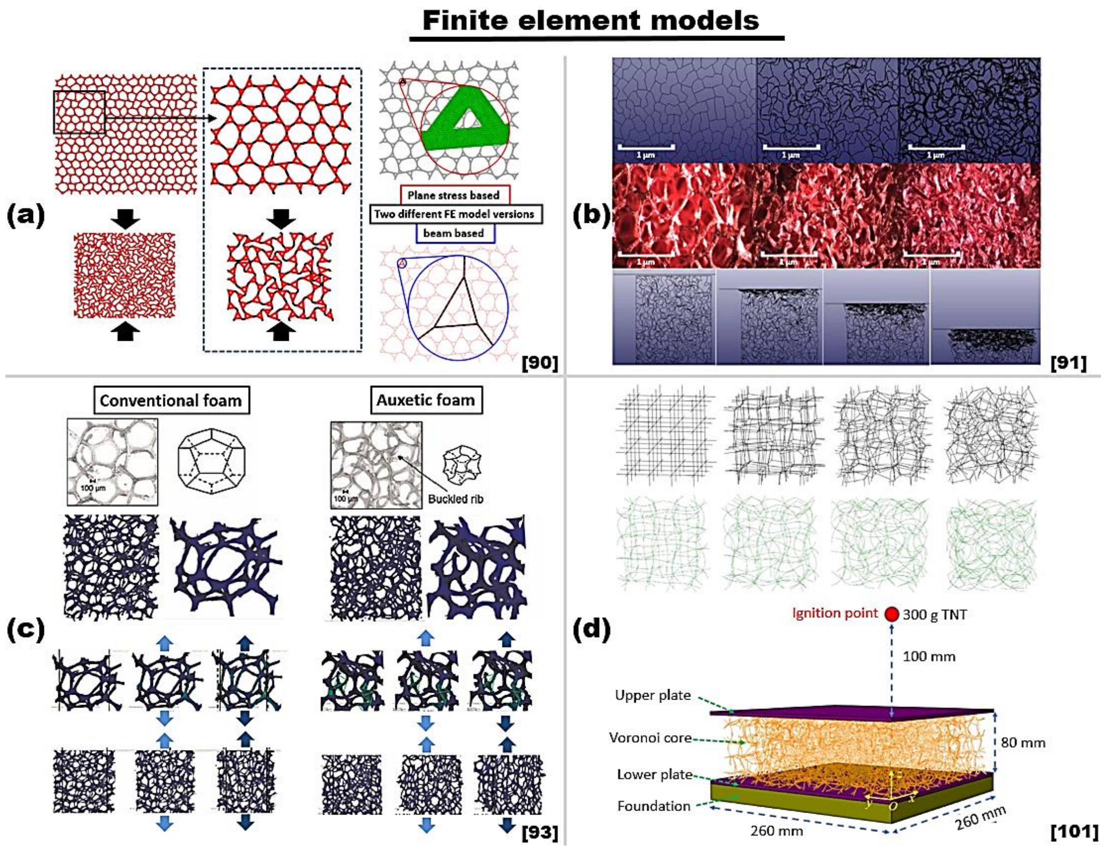

Figure. 14. FE models of auxetic foams in literature: (a) Two different FE model versions (plane stress based and beam based) for the proposed disordered auxetic structures [90], (b) 2D random cellular solid models based on a modified Voronoi tessellation technique for simulating the compression of copper foam [91], (c) microstructurally faithful FE models created from the reconstructed 3D tomography data [93], and (d) 3D isotropic auxetic foam core for blast resistance in FEA software by using random Voronoi structures [101], the structures can be generated by using different randomness (upper black ones) and tri-axial compression ratio (lower green ones).

4. Mechanical properties of auxetic foams

The most particular property of auxetic foams is the possession of negative Poisson's ratio ν, which is directly related, according to the classical theory of elasticity [102], to the Young's modulus E, the bulk modulus K (or resistance to changes to volume due to the application of a hydrostatic pressure) and the shear modulus G (or resistance to shear surface forces) in an isotropic material. The variation of the Poisson's ratio can significantly affect the mechanical behavior of the material. In an isotropic material with a constant E, if ν approaches - 1, the shear modulus G theoretically approaches to infinity, i.e., such material could be easily compressed but hard to shear.

$$G = \frac{E}{2(1+\nu)} \tag{1}$$

$$K = \frac{E}{3(1-2\nu)} \tag{2}$$

$$E = \frac{9KG}{(3K+G)} \tag{3}$$

$$\nu = \frac{3K - 2G}{2(3K + G)} \quad (4)$$

Though auxetic foams are highly anisotropic [15, 19, 97, 99, 103-105] and other relations between engineering constants need to be applied within the framework of classical elasticity to predict the behavior of anisotropic auxetics [106-108], auxetic foams show indeed better indentation shear resistance though the Young's modulus is smaller (lower *E*) than conventional ones [19, 31, 38, 45, 83, 108, 109]. The shear modulus in quasi-isotropic auxetic open cell foams can be well approximated using the formulas related to classical isotropic elasticity [110], but the shear stiffness of transverse isotropic auxetic foams has a different behavior [111]. The shear moduli vary between 10 - 38 kPa measured with a pure shear test [110] and 30 - 60 kPa via 3 point / 4 point bending tests [111], with the latter measurements taken at higher strain rates.

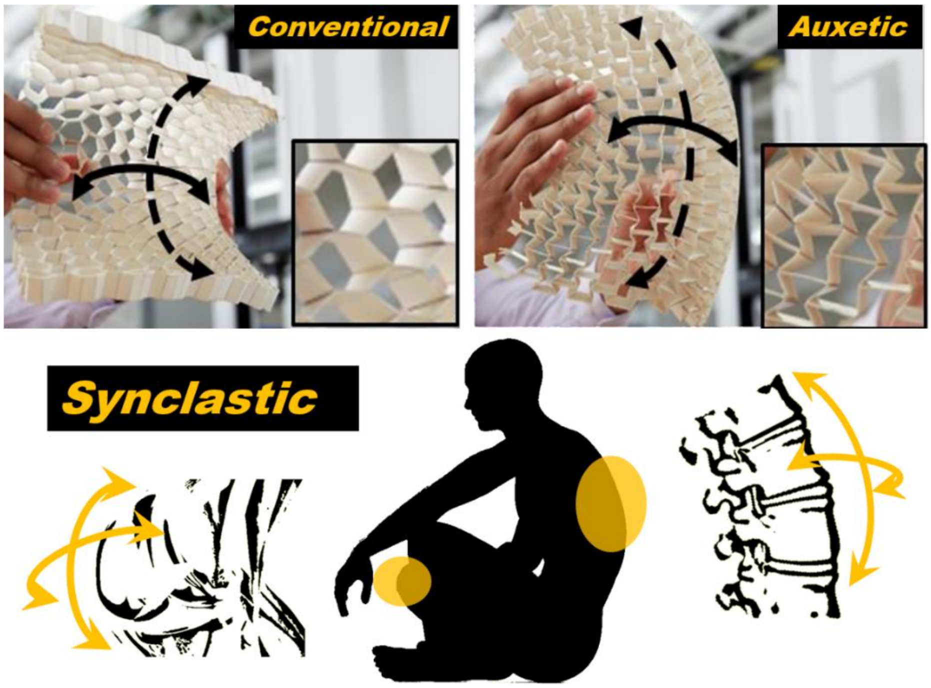

Figure. 15. Synclastic (dome-shaped) curvature behavior of materials with a negative Poisson's ratio, and drawing pictures present the ergonomic of this behavior (Images courtesy Andrew Alderson).

In terms of foam applications, the mechanical properties of stiffness (deformation resistance), hardness (indentation resistance) and toughness (fracture resistance) are very important. Auxetic foams also possess peculiar characteristics like the synclastic (dome-shaped) curvature (**Figure. 15**) [15, 19], reduction of vibration transmissibility (**Figure. 16**) [112], acoustic absorption (**Figure. 17**) [108, 112-118] and variable permeability (**Figure. 18**) [82, 119] Auxetic foams could also be made reversible, which means that the foams can be converted to their original state by a reforming process, i.e., they exhibit shape memory. (**Figure. 19**) [36, 43, 44, 54, 67, 74, 120, 121].

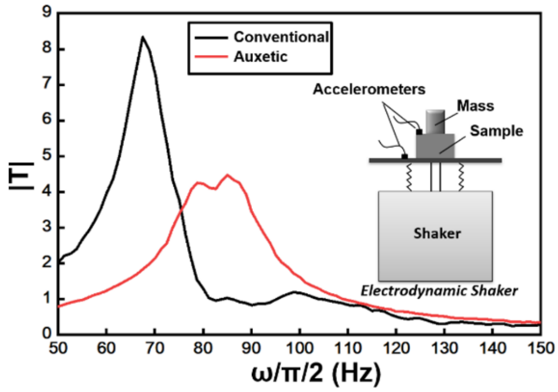

Figure. 16. Comparison between the vibration transmissibility (|T|) of conventional and auxetic foams between 49 and 150 Hz at low amplitude vibrations via electrodynamic shaker excitations (Data replotted from [112]).

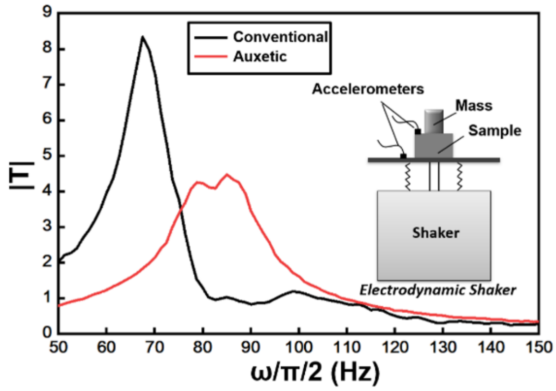

Figure. 17. Comparison of the frequency-dependent acoustic absorption between conventional and auxetic foams measured via acoustic impedance tube (Data replotted from [112]).

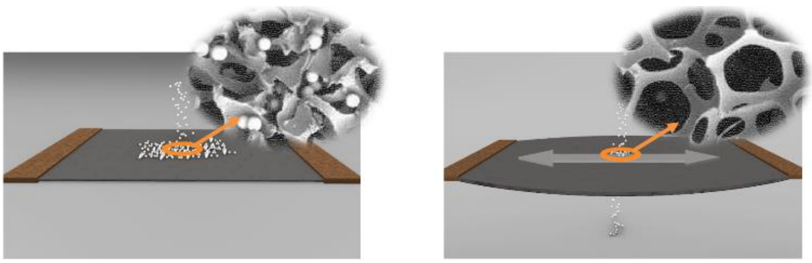

Figure. 18. Illustration of permeability tests with glass beads with auxetic foams, the foam pores can be enlarged by stretching (Images from [119]).

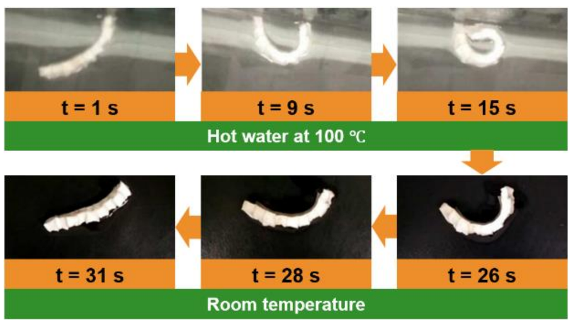

Figure. 19. Shape memory behavior of auxetic PE foam (Adopted from [36]).

4.1 Stiffness

The stiffness k is a parameter used to assess the deformation resistance offered by an elastic body:

$$k = \frac{F}{\triangle l} \tag{5}$$

Where F is the force applied on the body and $\triangle l$ is the resulting deformation of the body. The stiffness and its evolution could significantly affect the EA and peak force under specific sets of loadings.

The stiffness of auxetic foams is in general lower than their conventional counterpart at lower compression strains (**Figure. 20**) [30]. Chan and Evans [122] thought conventional foams need to overcome the stiffness of their hexagonal pristine structure before the ribs become bent, whereas the ribs of auxetic foams are already bent when testing. Such phenomenon was also found by Bhullar [123], and the paper proposed that the lower stiffness at small strains could be beneficial to biomedical implants.

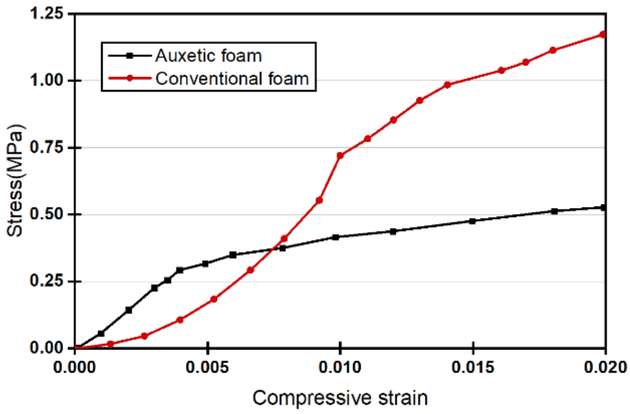

Figure. 20. Initial part of compressive strain-stress curves of auxetic foam and conventional foams (Data replotted from [30]).

As the compression increases, auxetic foams shrink laterally due to their unique re-entrant structure, making the density and stiffness increase significantly. Such phenomenon can be seen in other auxetic structures and nowadays the stiffness control [124] during the loading process has become a research point. On the contrary, conventional ones expand laterally and the density and stiffness in general feature more limited changes. Auxetic foams will therefore tend to be denser and stiffer than conventional ones at higher compression strains. A lower stiffness of auxetic foams could only be observed in a very small strain and hardly exists in samples having small scale pores. Foam materials are widely used to undergo large deformation, so the lower stiffness in the very beginning part could be negligible in most applications, although stiffness at small strain is also a parameter that affect the static indentation of foams and the comfort provided in cushioning. The stiffness of auxetic foams is sensitive to strain rate: the higher the strain rate be applied, the stronger the stiffening effect [20, 125] (**Figure. 21**).

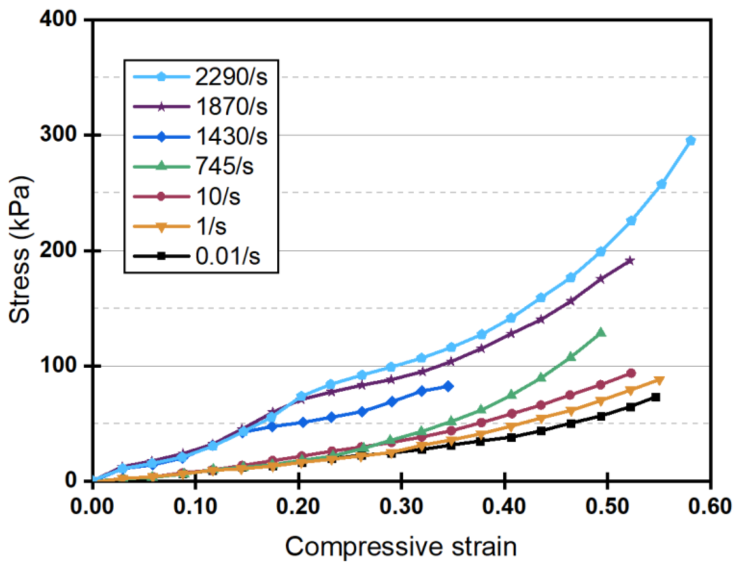

Figure. 21. Compressive strain-stress curves of auxetic PU foam at various strain rates (Data replotted from [20]).

4.2 Hardness

The hardness of foam materials is one of the representative parameters to evaluate their indentation resistance. The increased hardness of auxetic foams could be also predicted from the perspective of the classical elasticity theory, the relationship of hardness (*H*) and Poisson's ratio (ν) is given by:

$$H \propto= \left[\frac{E}{(1-\nu^2)}\right]^{\gamma} \tag{6}$$

Where *E* is the Young's modulus, γ is 1 under uniform load or 2/3 under concentrated load. When the ν approaches -1, the stiffness approaches to infinity.

Superior hardness of structures with a negative Poisson's ratio was reported in previous experiments [126-128]. Auxetic materials feature a unique type of deformation under indentation: the material around the loading area will tend to concentrate towards the impact point, causing a significant increase of local hardness. On the contrary, materials with positive Poisson's ratio would expand outwards from the impact point in similar loading conditions, making indentation easier (**Figure. 22**). This indentation resistance behavior has also been experimentally observed in auxetic foams [45, 47, 117, 122, 129-135].

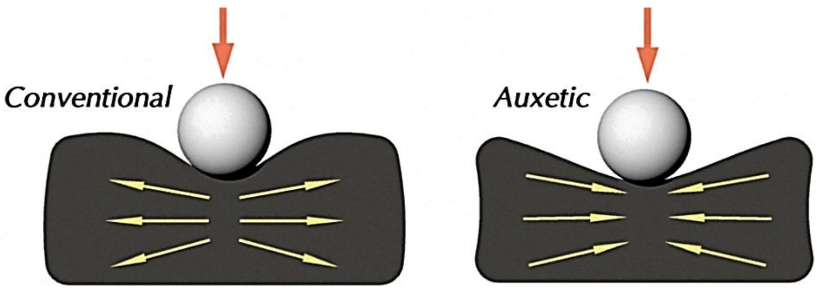

Figure. 22. Inner reactions under indentation of conventional (left) and auxetic foam (right).

Lisiecki *et al.* [51] argued that auxetic foams produced via the mechanic-chemic-thermal process are not suitable for impact mitigation due to their tendency of becoming denser under indentation or compression. Those authors performed quasistatic and drop tests, and indicated the higher deceleration and smaller impact hammer displacements at an equivalent static pressure of 12.3 kPa as evidence for their conclusions (**Figure. 23**).

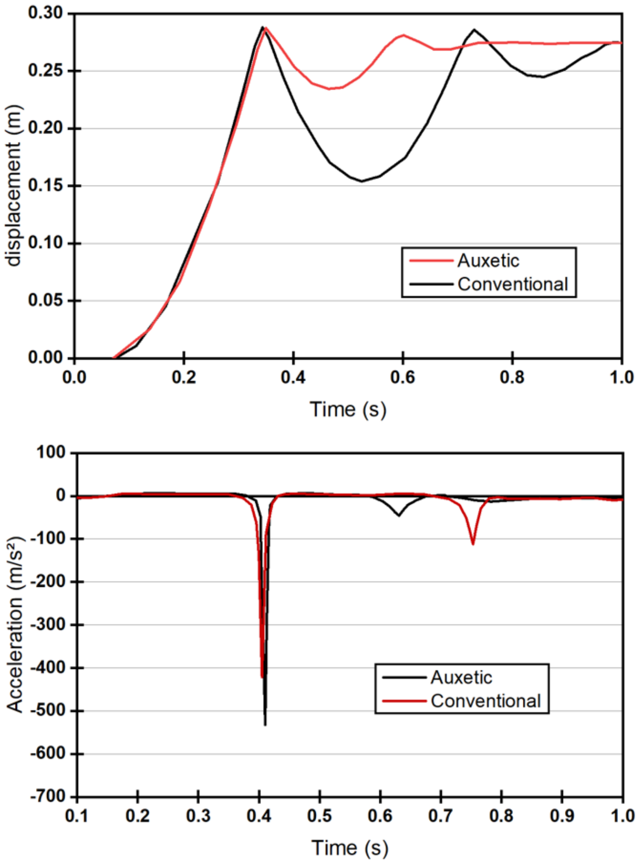

Figure. 23. Time histories of the hammer displacement (top) and acceleration (low) on auxetic and conventional foams for an equivalent static pressure of 19.6 kPa (Data replotted from [51]).

Soft foams may however bottom out under indentation [112, 136], slightly higher stiffness of auxetic foams may therefore provide more comfort as a cushion. Lakes and Lowe [71] noted that the volumetric compression ratio (or the final density) is critical to obtain an optimal performance under indentation in auxetic foams. Measurements of pressure distributions on PU foam cushions were performed by those Authors, and the results showed that the re-entrant foam at densities between 0.032 and 0.064 g/cm^3 performed better (i.e., lower maximum seating pressure) than conventional foam samples at comparable density. The auxetic foam material also wraps around the indenter under indentation, which provides a more uniform stress distribution and a reduced pressure concentration [71, 136, 137]. Further studies of Allen *et al.* [137] and Duncan *et al.* [138] showed that the peak accelerations (synchronized with the maximum deformation) of flat indentors used in drop tests on thermoformed-mechanical auxetic foams are smaller than in conventional ones under low-kinetic energy impact conditions. This indicated that those auxetic foams are promising for applications like cushions and pads (**Figure. 24**).

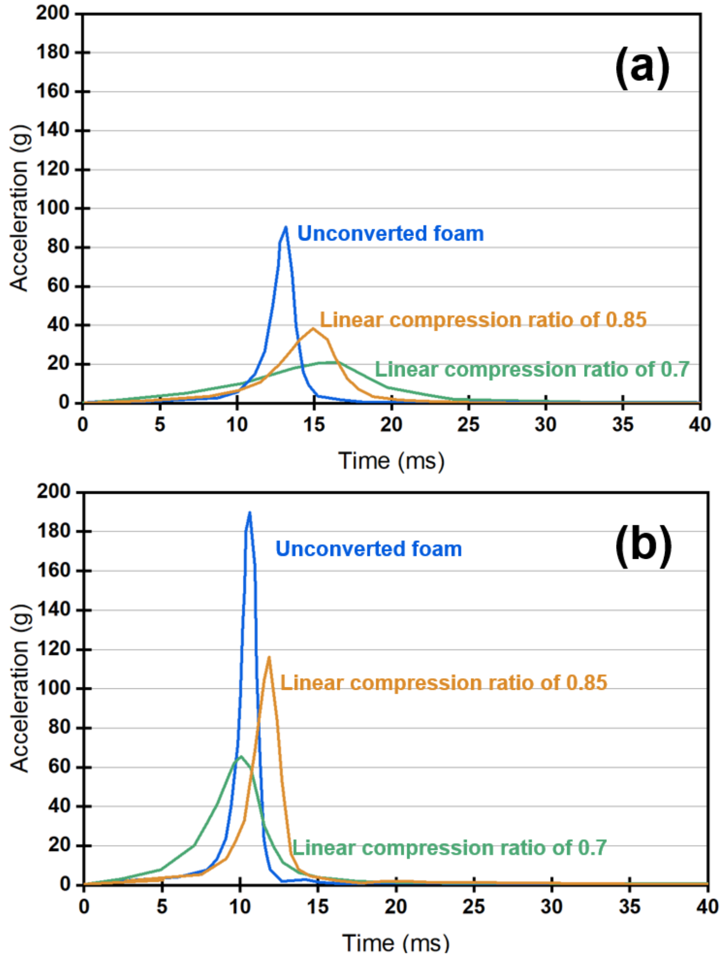

Figure. 24. Time histories of the acceleration for the flat indenter used in drop tests on R45FR foam at (a) 2 J and (b) 4 J of kinetic energy (Data replotted from [137]).

4.3 Toughness

Toughness indicates the ability of a material to resist fracture, and it is also a parameter adopted in crashworthiness designs [113, 139-141]. Toughness is in general critical for materials used in packaging and protection and it is measured by the area underneath the load-displacement or strain-stress curve. That area is also the value EA, while the specific energy absorption (SEA) indicates the energy absorbed per unit mass of the structure. These two parameters could be calculated as follows [142, 143]:

$$EA(d) = \int_0^d F(x)\,dx \tag{7}$$

$$SEA(d) = \frac{EA(d)}{m} \tag{8}$$

In those equations *d* is the crushing distance, *F* is the crushing force and *m* is the mass of the structure.

The parameters EA and SEA can be determined from quasi-static mechanical tests. Under quasi-static loading, auxetic foams absorb more energy than their conventional counterparts [40, 51, 54, 69, 101, 131, 132, 144-148]. A comparison of compression properties between auxetic foams and PPR (Positive Poisson's ratio) foams in ref. [54] is presented below as an example in **Figure. 25**.

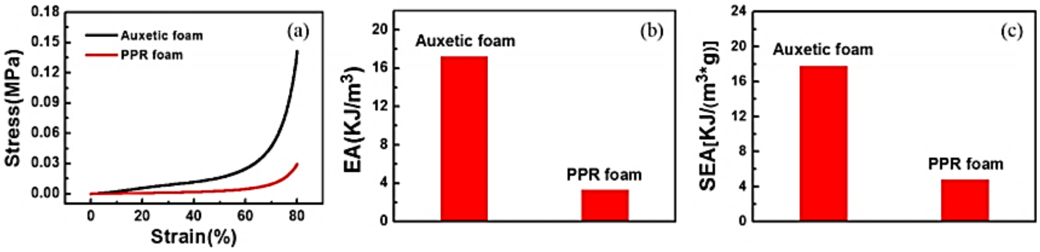

Figure. 25. Compression of auxetic and the PPR foams: (a) compressive stress-strain curve, (b) EA values for the auxetic and the PPR foams and (c) SEA for the auxetic and the PPR foams [54].

Mohsenizadeh and his group tested a series of auxetic foam-filled square tubes under both quasi-static and crushing tests with loading velocity of 1.5 m/s [139-141]. The EA value of the tube increases as the auxeticity of foam filler increases. The works of Scarpa *et al.* [80, 113] recorded the time histories of load and displacement in auxetic and conventional foams under high strain rate compression (**Figure. 26**). The time histories related to the auxetic foam demonstrated a better consistency, indicating a significantly improved resilience of the auxetic foam compared to the pristine conventional foam samples.

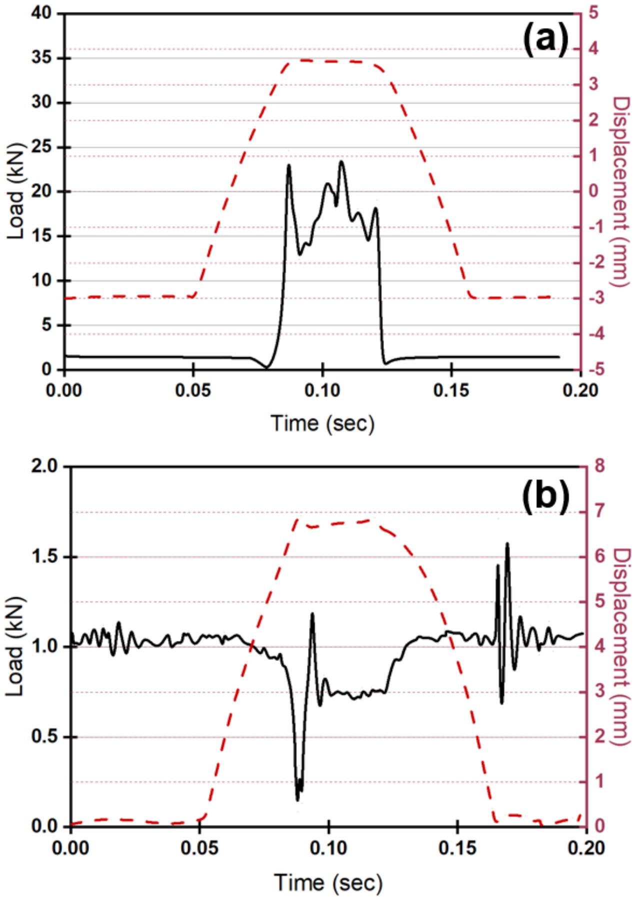

Figure. 26. Time histories of displacements and loads for (a) auxetic and (b) conventional foams under dynamic crushing loading conditions (cam plastometer) at 15 s^{-1}. The full curve represents the force history and the broken curve represents the displacement history (Data replotted from [113]).

A series of fatigue tests were carried out by Bezazi and Scarpa [131, 149] to investigate the toughness, stiffness loss and damping capacity of auxetic foams under cyclic loading (**Figure. 27**). In those studies, the maximum load F was recorded as a function of the number of cycles N and normalized by the maximum load F_0 obtained during the first cycle. The loading level r was defined as the ratio between the maximum displacement at a particular level to the displacement at failure. A larger energy dissipation was observed in the displacement-load curve of the first cycle and the auxetic samples show a lower stiffness degradation (rigidity loss) (F / F_0) after a large number of cycles compared to the parent conventional ones.

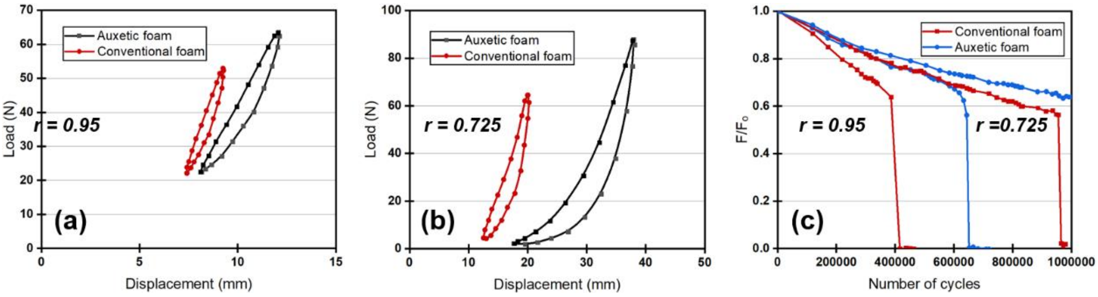

Figure. 27. Direct comparison between first cycle hysteresis loops for auxetic and conventional foams at different loading levels of (a) $r = 0.95$ and (b) $r = 0.75$; (c) Stiffness degradation versus number of cycles for the two types of foams at different loading levels: $r = 0.95$; $r = 0.725$ (Data replotted from [131]).

Another less documented but important parameter is the fracture toughness evaluated by Choi and Lakes [31] in auxetic copper foams, with significant improvements compared to the conventional copper foam version. Although those enhanced properties in fracture are promising in terms of the load-bearing applications, to the best knowledge of the authors of this review, no other work has focused on the fracture toughness of auxetics yet.

5. Applications of auxetic foams

Auxetic foams are in essence transformed from traditional porous materials. The transformation leads to a set of very desirable properties that conventional foams do not possess. It is therefore reasonable to consider auxetic foams either as a replacement of conventional porous materials, or as the basis of completely new designs to exploit their ad-hoc properties. Foam materials are commonly used as fillers for cushion and auxetic foams, compared to conventional ones, may further improve comfort and reduce the risk of pressure sores because of their EA [51] and pressure reduction [71, 136, 150]. These superior properties are also highly attractive for protective equipment in sports applications such as pads or mats [51, 71, 136], gloves [144], helmets [132, 151], spots shoes [132] and snow-sport safety devices (body armour and crash barrier) [145].

Several thin-walled tubes with auxetic foam core have been designed by Mohsenizadeh et al. [140, 141, 152]. Compared to the control group made with conventional foam, the compression induced shrinkage (density increasing) of the auxetic foam core provides enhanced EA and crashworthiness (**Figure. 28**). Recently, Zhang et al. proposed a series of auxetic tubes with superior mechanical properties [153, 154], compared with the ordinary tubes as the above-mentioned ones, such novel auxetic tubes could further enhance the mechanical performance of auxetic foam-filled tubular structures.

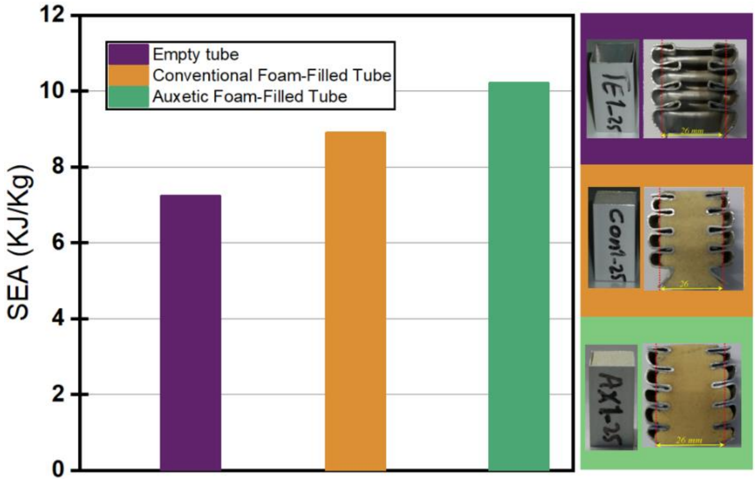

Figure. 28. SEA and sections of foam-filled tubes (Adapted from [153]).

Sandwich composite beams with auxetic foam core could bear large loading (high shear stress) under large deformations [111] and possess significant mechanical impedance with an interesting zero stiffness behavior [155] (**Figure. 29**). Depending on the type of application and loading, auxetic foams could be used to tailor the performance and the overall weight of the structural sandwich panel in which they are embedded. Zahra *et al.* [156] have described the manufacturing and characterization of cementitious polymer mortar-auxetic foam composites and showed that the embedding of the auxetic foam could avoid delamination and brittleness of the cement (**Figure. 30**). The unique deformation under compression (material concentration at compression area (**Figure. 22**)) endows auxetic foam with enhanced resistance for fracture. Such outstanding performances are potential in the engineering field. Except for axial compression, it is also worth researching to test auxetic structures under complicated loading conditions.

Recent progress in seismic metamaterial was reported by Huang *et al.* [157], a series of numerical simulations certified the positive function of auxetic foams as the shell to attenuate Lamb wave, realizing the generating of ultra-low frequency bandgap (**Figure. 31**). Their work is significant to researchers who are devoted to the wave or sound isolated function of auxetic foams. Such lightweight functional material is also promising in civil engineering and disaster prevention and mitigation.

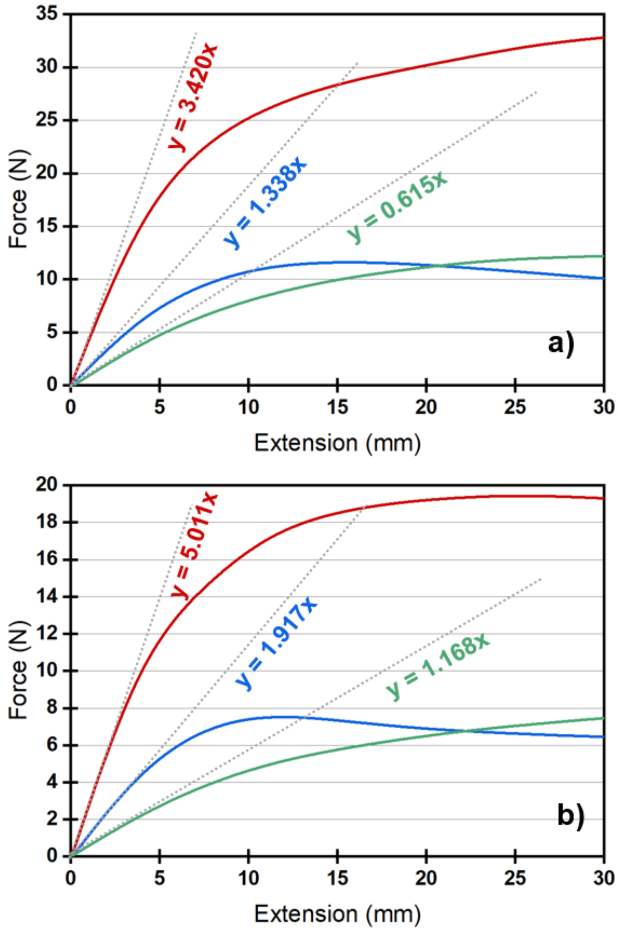

Figure. 29. Force versus central deflection for a) 3-point and b) 4-point bending test on sandwich panels with different foam cores. Green, auxetic; blue, conventional thin; red, conventional thick. The slope of dashed lines represents tangent stiffness of the proposed foam cores (Data replotted from [111]).

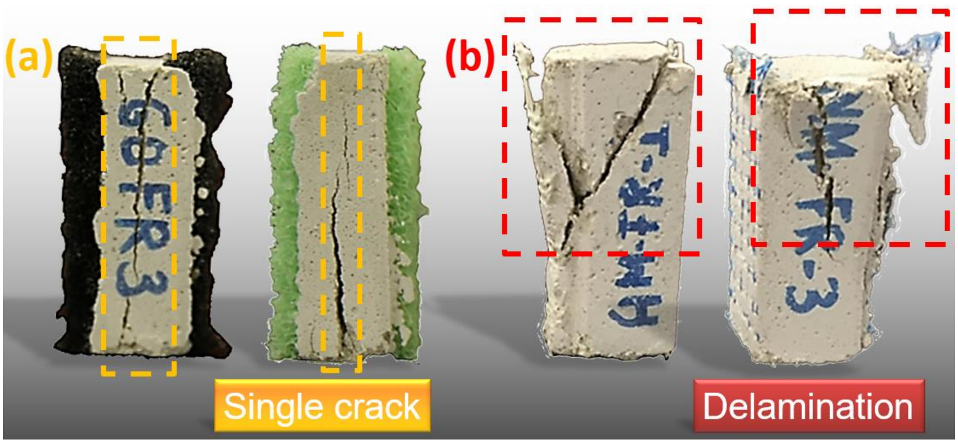

Figure. 30. Cracking characteristics of (a) cementitious polymer mortar - auxetic foam composites and (b) cementitious polymer mortar-PPR fibreglass mesh composites (Adapted from [156]).

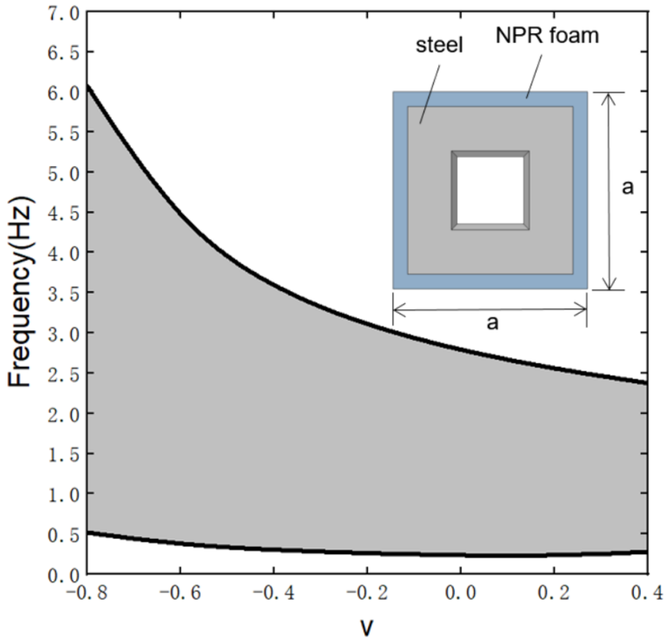

Figure. 31. The novel seismic metamaterial based on auxetic foam and the effect of Poisson's ratio of auxetic foam on the first complete bandgap (Adapted from [157]).

For investigating and utilizing the behavior of auxetic foams under torsion, semi-auxetic rods have been designed by Lim [158]. This novel design of rods produces unique mechanical behaviors under torsion for potential use as smart structures with different responses under multivariate loading. Concentric auxetic-conventional foam rods with high modulus adhesive at the interface have been modeled using an analytical approach to investigate the effect of the adhesive on the overall auxeticity of the system [159]. As for bending condition, where auxetic materials present the characteristics of synclastic curvature, Mohanraj *et al.* [150] designed a hybrid composite support for people with multiple sclerosis, consisting of an auxetic open cell foam liner and curved thermoplastic plates with rhomboidal perforations. Different types of material substrates allowed in this design can contribute to reducing the capital costs of development and increase the life cycle of the products for these particular biomedical applications. Synclastic curvature is an ergonomic deformation mode to perfectly stick a human's head, dorsum and joints (**Figure. 15**). In that, the more uniform stress distribution provided by shape fitting could be also used as soft tissue implants in cartilage articulations and meniscus repair for knee prosthetics [123].

Honeycomb membranes with conventional and re-entrant cell geometries have been successfully fabricated and tested by Alderson *et al.* [160], re-entrant samples show an enhanced functional performance compared to conventional (hexagonal ones) ones for glass chromatography beads in applications related to filtration systems. Inspired by this unique property of auxetic structures, a series of studies on auxetic foams were performed by the group of Alderson [82, 119]. A variation of the pressure-drop and transport properties was also observed in auxetic foams, making the negative Poisson's ratio porous material appealing for sieving of beads of uniform diameter and air pressure-drop applications (**Figure. 18**). The dramatic change of pore size that auxetic open cell foams exhibit under mechanical loading (compact re-entrant pore to expanded hexagonal pore under stretching) can be useful to compensate the increase in pressure-drop which arises due to increased filter fouling, flushing or altering the response of a filter or catalyst structure.

The large displacements given by the auxetic behaviour for a given applied load have been also highlighted by Scarpa *et al.* [113], and a proposal for using auxetic foams to enhance self-sensing structural components was there presented. This large deformation feature of auxetic foams was used to develop variable stiffness and shape hybrid negative Poisson's ratio PU-PE foams saturated with magnetorheological fluids (MRFs). These smart foam systems have shown tunability of the stiffness and magnetostrictive effects (up to 4 times stiffness increase by applying 0.2 T of magnetic field) [161, 162] and tunability of the electromagnetic and acoustic absorption of surface-coated MRF foams [115]. Auxetic open cell PU-PE foams seeded with carbonyl particles and magnetorheological fluids have also shown an increase of the acoustic absorption by a factor of ~ 7 compared to the pristine foam within the 1 kHz - 2.5 kHz bandwidth and the presence of a peak absorption of ~ 1 with the MRF that could be shifted by almost 500 Hz when applying magnetic fields between 0.1 T and 0.2 T [114].

As a soft material with significant lateral deformation under longitudinal loadings, auxetic foams are great candidates to serve as sensitive movement sensors. In 2013, Alderson *et al.* [163] introduced the term "piezomorphic" to describe mechanically-triggered shape change materials and proposed an elastic-gradient piezomorphic material (**Figure. 32**) made from PU foam and micro porous polymer (ex-PTFE). The piezomorphic material possesses both negative and positive Poisson's ratio regions and show a dramatic shape change triggered by the application of global and local stresses.

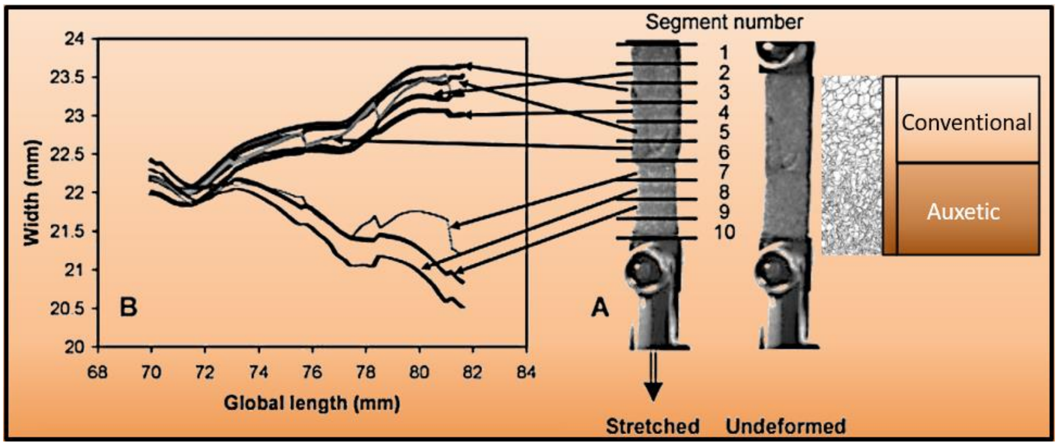

Figure. 32. Global length-width curves of different parts related to the elastic-gradient piezomorphic material (Adapted from [164]).

The piezomorphic behaviour could also be exploited to use auxetic foams as platforms to build sensors. The first contact-mode triboelectric self-powered strain sensor using an auxetic PU foam (**Figure. 33**) has been fabricated by Zhang *et al.* [164]. This sensor can be used in human body monitoring systems, self-powered scales to measure weight or in seat belts to measure the body movements on a car seat.

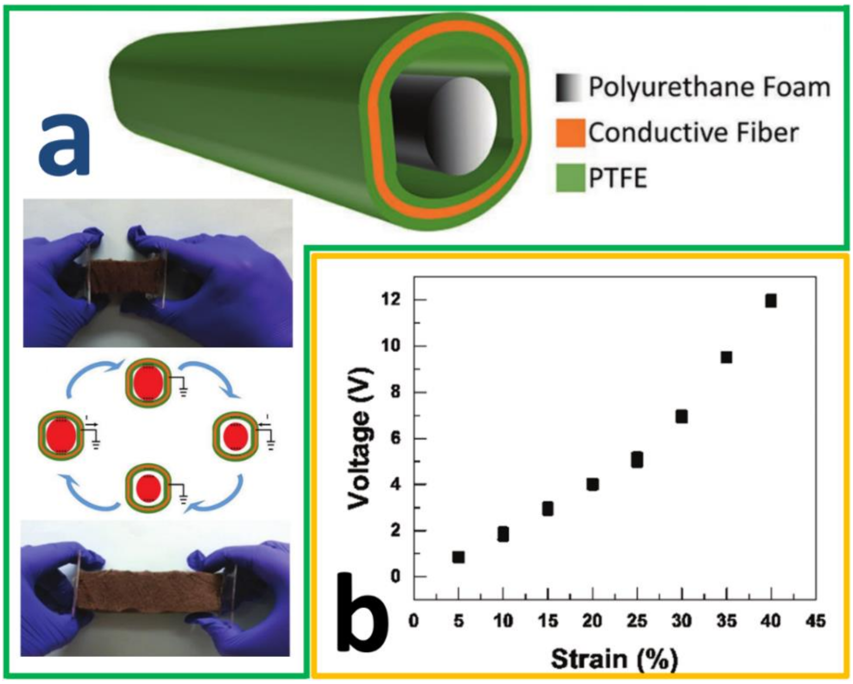

Figure. 33. (a) Schematics and (b) voltages under different tensile strains of the contact-mode triboelectric self-powered strain sensor (Adapted from [164]).

The porous structure in auxetic foam provides the space for conductive components to composite in, making auxetic foam itself with high electrical conductivity. Ahmed *et al.* [165] have developed an AgNW (silver nanowire) - based auxetic foam sensor (**Figure. 34**). This device has been trialed for air pressure detection and three-dimensional sensing. The AgNW-based auxetic foam sensor possesses both improved piezoresistive sensitivity and stability in air or water. The device also shows repeatable and reliable sensing performance under cyclic loading or unloading situations. Other potential applications of this device as mentioned in the paper include sportswear, safety gears, filtration and flow detection, smart healthcare foams and prosthetic liners.

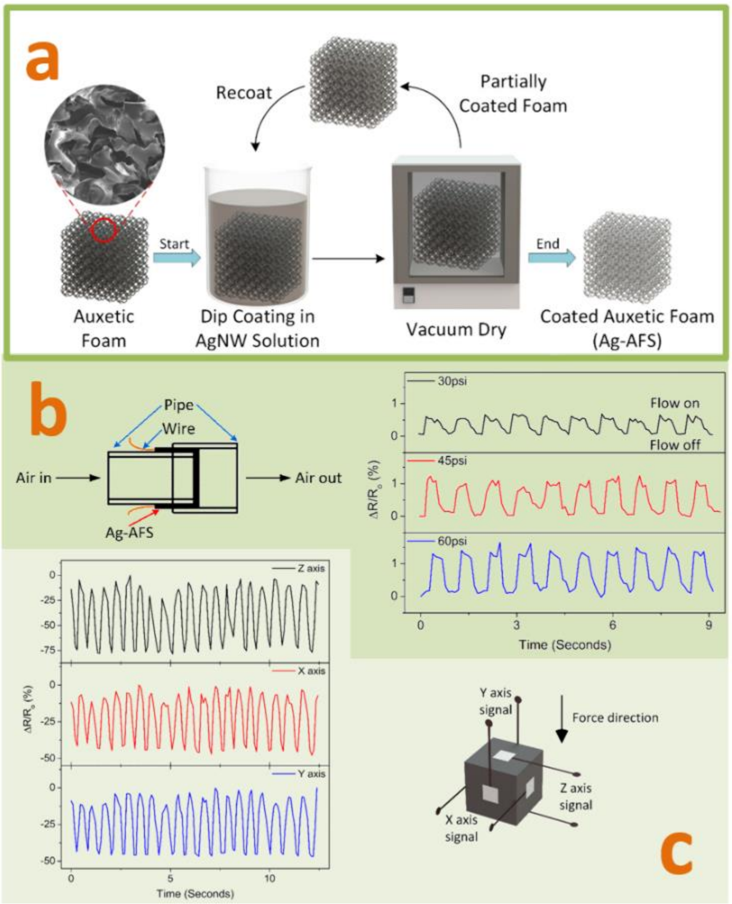

Figure. 34. Schematics of (a) fabrication of the AgNW sensor and applications to (b) air pressure detection and (c) three-dimensional sensing (Adapted from [165]).

Another interesting design of a strain-gauge sensor has been proposed on a combination of multiwalled carbon nanotube/polydimethylsiloxane (MWCNT/PDMS) substrate fabricated on an open-cell PU auxetic foam by Malfa *et al.* [166] (**Figure. 35**). This porous sensor could be used to integrate flexible electrode and soft robotics designs.

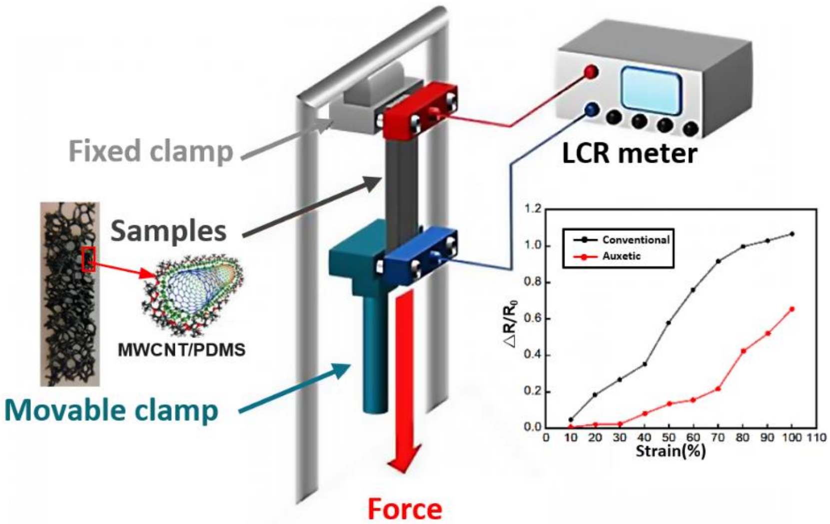

Figure. 35 . Flexible carbon nanotubes-based auxetic sponge electrode for strain sensing (Adapted from [166]).

6. Challenges and perspectives

Auxetic foams could be a potential alternative to conventional foams in applications where special deformation mechanisms of the foam material play a significant role. However, most of the potential applications are limited by the substantial lack of scale-up manufacturing methodologies to produce large auxetic foam samples. The development of feasible, effective and low-cost ways to manufacture large specimens of negative Poisson's ratio foam samples is crucial to future commercialization. Methodologies of utilizing chemical reactions to soften foam ribs [50, 51] or decrease the required temperature during conversion [36, 53-55] are beneficial in eliminating heat transfer problems. Therefore, further investigation of the chemical properties of foam materials and the development of chemical conversion equipment are necessary for manufacturing scale-up of auxetic foams. Some auxetic foam specimens reported in open literature do not maintain stable mechanical properties in the long term, with samples also recovering their original shape after a period of time, or being re-subjected to heating (shape memory effect [43, 44, 121]). One could however take advantage of this feature for some specific applications (for example: if maximum volume application is an issue, one could use auxetic foams in situations where the volume available is greatly reduced, and make use of the shape memory effect to restore the porous material to its pristine side when volume available is not anymore an issue). The long-term stability of the mechanical properties is however paramount in most engineering applications (cushions and pads, for example). The further development of manufacturing procedures and methodologies to control the recovery and stability of auxetic foams would significantly improve the use of negative Poisson's ratio foams in the design at higher technology readiness levels.

A considerable number of geometric models with different deformation mechanisms [15, 30, 42, 49, 77, 79-83, 85, 87-90, 126, 134] have been proposed to simulate auxetic foams in the past decades. Those models provide explanations and predictions of specific mechanical properties to some extent. However, as a material with high heterogeneity [104] and anisotropy [126], auxetic foams cannot be accurately described by deterministic geometric modeling only. Image-based techniques like SEM and CT are able to show real and detailed micro-structure of auxetic foams [36, 39, 49, 56, 73, 85, 93, 95, 96, 98]. The more systematic use of solid models extracted from μ-CT scans and converted into FE would increase the fidelity of the modelling of auxetic foams. There are however also some issues associated to high-fidelity FE simulations of auxetic foams extracted from CT scans. The first is the need of large numbers of μ-CT volumes to be extracted from different positions of the auxetic foam block. Little is known about the effective heterogeneity distributed within a negative Poisson's ratio foam, scans tend to be expensive and take long time to be performed, most of the data available are related to a single or very few scans inside the foam blocks. The limited number of scanned volumes inside the same block of auxetic foams limits the statistical validity of the topological information that can be extracted from imaging the microstructure of the foam itself. The second issue related to the use of FE with solid models extracted from foam scans is the fact that very little is known about the mechanical properties of the core polymer constituting the foams. Estimates of the Young's modulus from inverse identification of the PU in auxetic PU foams subjected to mechanical loading and other data from open literature vary between 10 MPa to ~250 MPa [34, 167-169]. Moreover, the simulated stiffness and/or stress-strain curves from the μ-CT scan FE models are heavily dependent upon the type of boundary conditions and loading applied, making any direct comparison with experimental curves especially obtained from homogenized auxetic foam samples quite problematic. Any technique developed to increase the number of high-fidelity scans in an affordable way and improve the reliability of the FE modelling in terms of core material properties and boundary conditions would significantly help the computational modelling of auxetic foams. Another approach that could offer some advantages in modelling statistically realistic auxetic foams is the use of 2D random models that show some similarity to the topology of negative Poisson's ratio cellular materials like Thiessen polygons (Voronoi diagrams) [170-173]. Quite interestingly, Li *et al.* [91] have shown that by using 2D Voronoi networks to simulate Cu copper foams subjected to strain hardening and biaxial compression, it is possible to predict the resulting Poisson's ratio and EA capacity of the real auxetic metal foams. The use of stochastic based tessellation for PU pristine foams based on Kelvin lattices or similar topologies and more in-depth information about the mechanics and shape memory effect of the core PU could be instrumental to create a digital twin of the manufacturing process of auxetic foams. Lakes *et al.* also introduced Cosserat (micropolar) theory [174] for the analysis of materials with negative Poisson's ratios [108, 175, 176], stating that syntactic foams could be regarded as classical ones apart from small deviations. Rueger and Lakes however found compelling experimental evidence of the existence of Cosserat torsion lengths and coupling due to size effects while testing the foams [177]. Gaspar *et al.* [178] developed a theoretical framework to predict the elastic properties of a material with contacting microstructure originally proposed by Koenders [179] and extending the previous formulation to continuum materials with auxetic behaviour and anisotropic heterogeneity. Ciambella *et al.* [180] and Rueger *et al.* [181] modeled auxetic open cell foams as continuum solids for the analysis of nonlinear elasticity within a modified Ogden hyperelastic anisotropic framework. Recently, the group of Montáns [182, 183] provided a series of extension of phenomenological linear theory, realizing the simulation of strain-stress relation and auxetic behaviour of auxetic foam through an accurate numerical methodology. Such methodology makes orthotropic materials not only feasible but also efficient (compared with FE analysis) simulated. However, the simulation processes of their works are carried on axial quasi-static loading only, some sophisticated loading conditions such as impact, crushing and cyclic loading are inescapable in applications, therefore are desirable to be simulated as well. Auxetic foams produced with the current manufacturing methodologies are difficult to simulate with high-fidelity continuum Cauchy classical elasticity models. The theoretical approaches discussed above are an indicator for the need to further develop more high-fidelity continuum theories and therefore to realistically simulate the deformation mechanisms and size effects observed in real foams.

Another interesting and promising concept is to engineer the large lateral deformations triggered by axial loading in piezomorphic foams to design and fabricate sensors [163-166]. Soft sensors have significant potential in applications like soft robotic, biomedical and behavioral sensing, smart belts (**Figure. 36**) and smart clothing. Piezomorphic materials [34] could be also used as actuator elements by enabling turning on/off of devices in response to stress-induced shape changes (**Figure. 36**). Other potential applications are in the smart bandage sector (drugs can be released when the bandage is stretched by the swelling of the wound), adaptive airfoils (stress induced shape change), prosthetic limb lining (fit stump volume variations), bra cups (expand during vigorous exercise and/or periods of significant variations in breast size) and deployable/removable cores (easy to insert and hard to extract, a similar application of auxetic nails can be seen in ref. [184]).

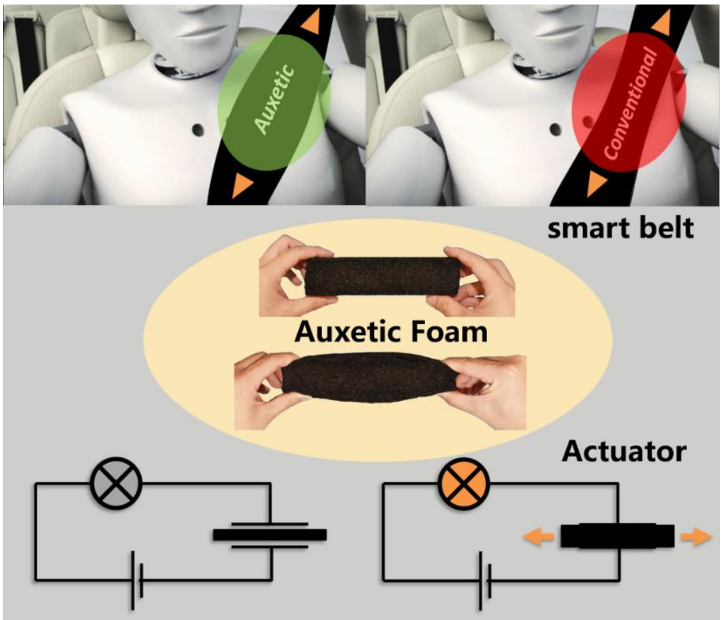

Figure. 36. Examples of potential applications utilizing the unique stress-induced shape change of auxetic foam materials (middle): smart belts (upper) and actuator elements (lower).

Composite materials and structures with auxetic foams are also promising for applications like complaint composites for prosthesis, impact and blast protection. Recently, composite structures with auxetic foams and cellular materials have been designed, modelled and built, showing interesting performances for energy [141, 152, 185] and shear resistance [19, 31, 38, 45, 83, 108, 109, 111]. Compared with other traditional core materials, auxetic foams tend however to possess a low stiffness. It would be therefore interesting to develop more rigid and lightweight auxetic foams with enhanced mechanical properties, both on the polymeric and metal foam side, as well as to explore hybrid combinations of auxetic foams and other more rigid materials or structures. Lightweight characteristics are also important. Auxetic foams are denser than their pristine conventional counterpart used for the production, depending on the volumetric compression ratio. While some specific mechanical properties are significantly enhanced compared to the conventional original foam, the comparison of the specific properties (i.e., density or weight averaged) between auxetic and conventional foams may not offer the same advantages as the direct ones. Besides, as a type of cellular material, auxetic foam is potential to be a candidate for matrix material, in which fluid or powder additions, such as graphene oxide [117] and Er [121], of which are easy to disperse and adhere to the foam ribs, i.e., forming composite foam materials (**Figure. 37**). Composite foams hold the superior properties provided by additional materials meanwhile retain the properties of foam materials themselves, many composite foams are still based on conventional foams [186-194], it is potential to convert those composite foams into auxetics, in that original foams could obtain triple functions.

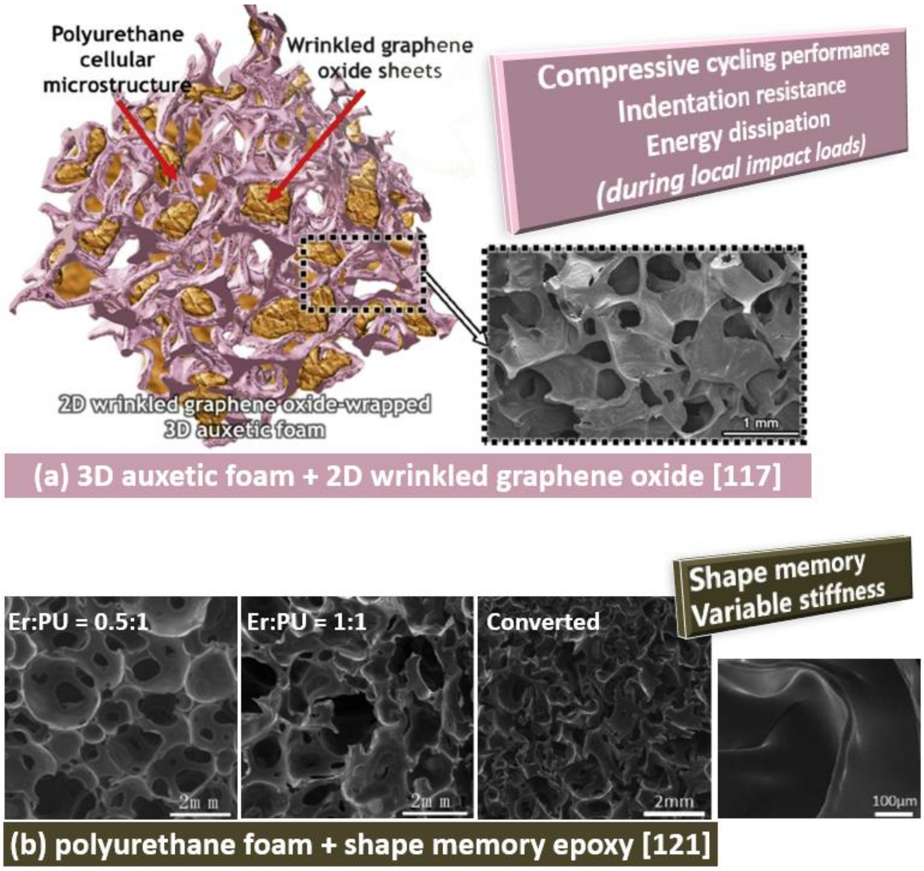

Figure. 37. Two kinds of auxetic composite foams of (a) 2D graphene oxide-wrapped auxetic PU foam and (b) shape memory composite foam, and their functional enhancements (Adapted from [117] and [121]).

A series of configurations made using auxetic frames and inclusions of conventional foam have been also investigated (**Figure. 38**) [195, 196]. In a broad sense, these configurations can be defined as hybrid auxetic by increasing the bulk properties of the composite with the foam matrix and using the auxetic lattice in a synergistic way to increase the EA and impact protection.

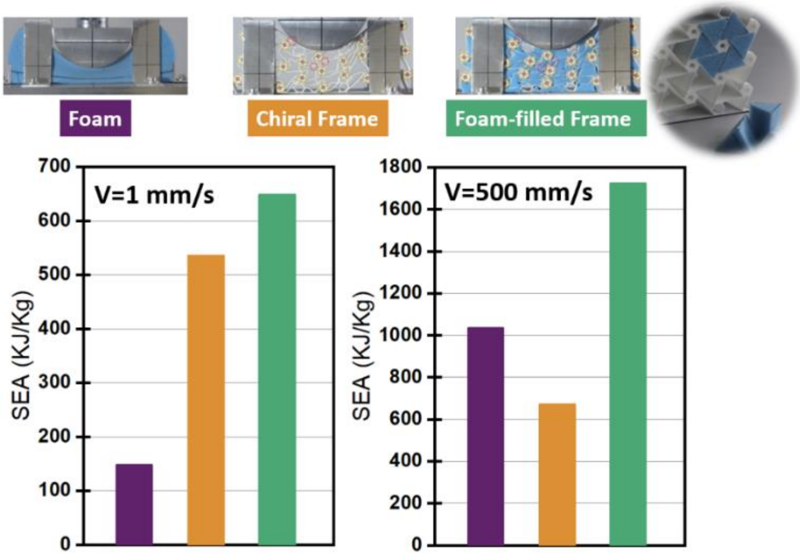

Figure. 38. EA performance of foam-filled auxetic structures tested for an indentation of 50 mm (Adapted from [196]).

In addition, rigid open-cell auxetic and metal foams could be used as scaffolds to build silicone [197], mortar [156], concrete and other similar high-performance composites. Random reticular structures of the foam scaffolds could contribute to oppose shear failure and fracture in these foam-based composites [156].

Another aspect to be considered and of increasingly significant importance is the environmental impact of auxetic foams, especially in view of scale-up manufacturing processes. All the manufacturing processes used to fabricate polymeric foams, in particular, necessity of either temperature and/or use of chemicals. Considering the contribution of tooling, molding and labor, detailed life cycle costs of the different manufacturing processes are needed to make the business and environmental case for the large-scale manufacturing of auxetic foams. The use of more bio-based polymers and products during the manufacturing is also an interesting aspect to be considered.

7. Conclusions

In this paper, the state-of-the-art of manufacturing, characteristics and applications of auxetic foams have been reviewed. Existing methodologies for the conversion of auxetic foams have been presented and focus has been put on the relations between the different possible manufacturing parameters and recommended optimal combinations of those. The micro-structure and deformation mechanisms in auxetic foams have been discussed, from theoretical unit cell models to more high-fidelity numerical ones based on geometry information extracted from imaging techniques. The mechanical properties of auxetic foams have been considered here in terms of stiffness, hardness and toughness, showing superior performance in loadings like indentation, impact, cyclic and vibroacoustic. Auxetic foams could represent enhanced alternatives to conventional foams in many applications where unusual deformation mechanisms of the foam material play a role. We have also provided a consistent number of examples of novel applications of auxetic ranging from biomedical, aerospace, filtration and sensing, to name a few. This paper also provides a discussion of existing challenges and future research directions to enhance the feasibility and the design space of auxetic foam materials and structures.

Acknowledgments

This work was supported by the National Natural Science Foundation of China (grant numbers 51978330, 51778283); National Natural Science Foundation for the Youth of China (grant number 51808286); Natural Science Foundation of Jiangsu Province (grant number BK20180710); and the Innovation Project for Graduate Student of Jiangsu Province (grant number KYCX20_1009). FS would like to acknowledge the support of the UK Engineering and Physical Sciences Research Council (EPSRC) EP/R032793/1 SYSDYMATS project. FS is also grateful to Dr Qicheng Zhang from the Bristol Composites Institute for the discussions about the FE modelling.

References:

[1] Fung YC. Foundations of Solid Mechanics. Prentice-Hall 1965:525.
[2] Voigt W. Allgemeine formeln für die bestimmung der elasticitätsconstanten von krystallen durch die beobachtung der biegung und drillung von prismen. Ann Phys 1882;252:398-416.
[3] Evans KE. Auxetic polymers: a new range of materials. Endeavour 1991;15:170-4.
[4] Love A. A treatise on the mathematical theory of elasticity 1892.
[5] Lees C, Vincent JFV, Hillerton JE. Poisson's ratio in skin. Biomed Mater Eng 1991;1:19-23.
[6] Veronda DR, Westmann RA. Mechanical characterization of skin-finite deformations. J Biomech 1970;3:111-24.
[7] Williams JL, Lewis JL. Properties and an anisotropic model of cancellous bone from the proximal tibial epiphysis. J Biomech Eng 1982;104:50-6.
[8] Baughman RH. Auxetic materials: avoiding the shrink. Nature 2003;425:667.
[9] Wojciechowski KW. Constant thermodynamic tension Monte Carlo studies of elastic properties of a two-dimensional system of hard cyclic hexamers. Mol Phys 1987;61:1247-58.
[10] Hou J, Zhao G, Zhang L, Wang G, Li B. High-expansion polypropylene foam prepared in non-crystalline state and oil adsorption performance of open-cell foam. J Colloid Interface Sci 2019;542:233-42.
[11] Wang G, Zhao G, Dong G, Mu Y, Park CB, Wang G. Lightweight, super-elastic, and thermal-sound insulation bio-based PEBA foams fabricated by high-pressure foam injection molding with mold-opening. Eur Polym J 2018;103:68-79.
[12] Tiuc AE, Nemeş O, Vermeşan H, Toma AC. New sound absorbent composite materials based on sawdust and polyurethane foam. Compos B Eng 2019;165:120-30.
[13] Rizvi A, Chu RK, Lee JH, Park CB. Superhydrophobic and oleophilic open-cell foams from fibrillar blends of polypropylene and polytetrafluoroethylene. ACS Appl Mater Interfaces 2014;6:21131-40.
[14] Zhou J, Guan ZW, Cantwell WJ. The impact response of graded foam sandwich structures. Compos Struct 2013;97:370-7.
[15] Lakes R. Foam structures with a negative Poisson's ratio. Science 1987;235:1038-40.
[16] Greaves GN, Greer AL, Lakes RS, Rouxel T. Poisson's ratio and modern materials. Nat Mater 2011;10:823-37.
[17] Ren X, Shen J, Tran P, Ngo TD, Xie YM. Design and characterisation of a tuneable 3D buckling-induced auxetic metamaterial. Mater Des 2018;139:336-42.
[18] Ren X, Shen J, Ghaedizadeh A, Tian H, Min Xie Y. Experiments and parametric studies on 3D metallic auxetic metamaterials with tuneable mechanical properties. Smart Mater Struct 2015;24:095016.
[19] Evans KE, Alderson A. Auxetic materials: Functional materials and structures from lateral thinking! Adv Mater 2000;12:617.
[20] Zhai X, Gao J, Liao H, Kirk CD, Balogun YA, Chen WW. Mechanical behaviors of auxetic polyurethane foam at quasi-static, intermediate and high strain rates. Int J Impact Eng 2019;129:112-8.
[21] Novak N, Vesenjak M, Ren Z. Auxetic cellular materials - A review. Mech Eng 2016;62:485-93.
[22] Susmita Naik RDD, C. N. Wani, and S. K. Giri. A review on various aspects of auxetic materials. AIP Conf Proc 2015:020004.
[23] Duncan O, Shepherd T, Moroney C, Foster L, Venkatraman P, Winwood K, et al. Review of auxetic

materials for sports applications: expanding options in comfort and protection. Appl Sci 2018;8:941.
[24] Kelkar PU, Kim HS, Cho KH, Kwak JY, Kang CY, Song HC. Cellular auxetic structures for mechanical metamaterials: A review. Sensors (Basel) 2020;20:3132.
[25] Saxena KK, Das R, Calius EP. Three decades of auxetics research - materials with negative Poisson's ratio: A review. Adv Eng Mater 2016;18:1847-70.
[26] Ren X, Das R, Tran P, Ngo TD, Xie YM. Auxetic metamaterials and structures: A review. Smart Mater Struct 2018;27:023001.
[27] Luo C, Han CZ, Zhang XY, Zhang XG, Ren X, Xie YM. Design, manufacturing and applications of auxetic tubular structures: A review. Thin-Walled Struct 2021;163:107682.
[28] Zhang J, Lu G, You Z. Large deformation and energy absorption of additively manufactured auxetic materials and structures: A review. Compos B Eng 2020;201.
[29] Critchley R, Corni I, Wharton JA, Walsh FC, Wood RJK, Stokes KR. A review of the manufacture, mechanical properties and potential applications of auxetic foams. Phys Status Solidi B 2013;250:1963-82.
[30] Friis EA, Lakes RS, Park JB. Negative Poisson's ratio polymeric and metallic foams. J Mater Sci 1988;23:4406-14.
[31] Choi JB, Lakes RS. Fracture toughness of re-entrant foam materials with a negative Poisson's ratio: experiment and analysis. Int J Fract 1996;80:73-83.
[32] Chen CP, Lakes RS. Holographic study of conventional and negative Poisson's ratio metallic foams: elasticity, yield and micro-deformation. J Mater Sci 1991;26:5397-402.
[33] Li D, Dong L, Lakes RS. The properties of copper foams with negative Poisson's ratio via resonant ultrasound spectroscopy. Phys Status Solidi B 2013;250:1983-7.
[34] Alderson K, Alderson A, Ravirala N, Simkins V, Davies P. Manufacture and characterisation of thin flat and curved auxetic foam sheets. Phys Status Solidi B 2012;249:1315-21.
[35] Allen T, Hewage T, Newton-Mann C, Wang W, Duncan O, Alderson A. Fabrication of auxetic foam sheets for sports applications. Phys Status Solidi B 2017;254:1700596.
[36] Fan D, Li M, Qiu J, Xing H, Jiang Z, Tang T. Novel method for preparing auxetic foam from closed-cell polymer foam based on the steam penetration and condensation process. ACS Appl Mater Interfaces 2018;10:22669-77.
[37] Chiang Fp. Manufacturing and characterization of an auxetic composite. In: TMS, editor. Supplemental Proceedings: Materials Processing and Interfaces 2012.
[38] Chan N, Evans KE. Fabrication methods for auxetic foams. J Mater Sci 1997;32:5945-53.
[39] Mohsenizadeh S, Ahmad Z, Alipour R, Majid RA, Prawoto Y. Quasi tri-axial method for the fabrication of optimized polyurethane auxetic foams. Phys Status Solidi B 2019;256:1800587.
[40] Duncan O, Foster L, Senior T, Allen T, Alderson A. A comparison of novel and conventional fabrication methods for auxetic foams for sports safety applications. Procedia Eng 2016;147:384-9.
[41] Sanami M, Alderson A, Alderson KL, McDonald SA, Mottershead B, Withers PJ. The production and characterization of topologically and mechanically gradient open-cell thermoplastic foams. Smart Mater Struct 2014;23:055016.
[42] Duncan O, Allen T, Foster L, Senior T, Alderson A. Fabrication, characterisation and modelling of uniform and gradient auxetic foam sheets. Acta Mater 2017;126:426-37.
[43] Bianchi M, Scarpa F, Smith CW. Shape memory behaviour in auxetic foams: Mechanical properties. Acta Mater 2010;58:858-65.
[44] Bianchi M, Scarpa F, Smith CW, Whittell GR. Physical and thermal effects on the shape memory behaviour of auxetic open cell foams. J Mater Sci 2010;45:341-7.
[45] Martz EO, Lee, T., Lakes, R. S., Goel, V. K., & Park, J. B. . Re-entrant transformation methods in closed cell foams. Cell Polym 1996;15:229-49.
[46] Bianchi M, Scarpa F, Banse M, Smith CW. Novel generation of auxetic open cell foams for curved and arbitrary shapes. Acta Mater 2011;59:686-91.
[47] Zhang Q, Lu W, Scarpa F, Barton D, Lakes RS, Zhu Y, et al. Large stiffness thermoformed open cell foams with auxeticity. Appl Mater Today 2020;20:100775.
[48] Najarian F, Alipour R, Shokri Rad M, Nejad AF, Razavykia A. Multi-objective optimization of converting process of auxetic foam using three different statistical methods. Measurement 2018;119:108-16.
[49] Smith CW, Grima JN, Evans KE. A novel mechanism for generating auxetic behaviour in reticulated foams: Missing rib foam model. Acta Mater 2000;48:4349-56.
[50] Grima JN, Attard D, Gatt R, Cassar RN. A novel process for the manufacture of auxetic foams and for their re-conversion to conventional form. Adv Eng Mater 2009;11:533-5.
[51] Lisiecki J, Błażejewicz T, Kłysz S, Gmurczyk G, Reymer P, Mikułowski G. Tests of polyurethane foams

with negative Poisson's ratio. Phys Status Solidi B 2013;250:1988-95.
[52] Lisiecki J, Nowakowski D. The Impact of Technology on Poisson’s Ratio of Auxetic Polyurethane Foams. Aviat Adv Maint 2018;41:119-60.
[53] Li Y, Zeng C. Room-temperature, near-instantaneous fabrication of auxetic materials with constant poisson's ratio over large deformation. Adv Mater 2016;28:2822–6.
[54] Fan D, Shi Z, Li N, Qiu J, Xing H, Jiang Z, et al. Novel method for preparing a high-performance auxetic foam directly from polymer resin by a one-pot CO2 foaming process. ACS Appl Mater Interfaces 2020;12:48040-8.
[55] Duncan O, Allen T, Birch A, Foster L, Hart J, Alderson A. Effect of steam conversion on the cellular structure, Young’s modulus and negative Poisson’s ratio of closed-cell foam. Smart Mater Struct 2021;30:015031.
[56] Critchley R, Corni I, Wharton JA, Walsh FC, Wood RJK, Stokes KR. The preparation of auxetic foams by three-dimensional printing and their characteristics. Adv Eng Mater 2013:980-5.
[57] Jayavardhan ML, Doddamani M. Quasi-static compressive response of compression molded glass microballoon/HDPE syntactic foam. Compos B Eng 2018;149:165-77.
[58] Osman MM, Shazly M, El-Danaf EA, Jamshidi P, Attallah MM. Compressive behavior of stretched and composite microlattice metamaterial for energy absorption applications. Compos B Eng 2020;184.
[59] Curd ME, Morrison NF, Smith MJA, Gajjar P, Yousaf Z, Parnell WJ. Geometrical and mechanical characterisation of hollow thermoplastic microspheres for syntactic foam applications. Compos B Eng 2021;223.
[60] D'Auria M, Davino D, Pantani R, Sorrentino L. Magnetic field-structuring as versatile approach to shape the anisotropic mechanical response of composite foams. Compos B Eng 2021;212.
[61] Singh AK, Shishkin A, Koppel T, Gupta N. A review of porous lightweight composite materials for electromagnetic interference shielding. Compos B Eng 2018;149:188-97.
[62] Jiang H, Coomes A, Zhang Z, Ziegler H, Chen Y. Tailoring 3D printed graded architected polymer foams for enhanced energy absorption. Compos B Eng 2021;224.
[63] Song J, Wang Y, Zhou W, Fan R, Yu B, Lu Y, et al. Topology optimization-guided lattice composites and their mechanical characterizations. Compos B Eng 2019;160:402-11.
[64] Meng J, Liu T-W, Wang H-Y, Dai L-H. Ultra-high energy absorption high-entropy alloy syntactic foam. Compos B Eng 2021;207.
[65] Wang Q, Li Z, Zhang Y, Cui S, Yang Z, Lu Z. Ultra-low density architectured metamaterial with superior mechanical properties and energy absorption capability. Compos B Eng 2020;202.
[66] Wang Y, Lakes R, Butenhoff A. Influence of cell size on re-entrant transformation of negative Poisson's ratio reticulated polyurethane foams. Cell Polym 2001;20:373-85.
[67] Choi JB, Lakes RS. Non-linear properties of polymer cellular materials with a negative Poisson's ratio. J Mater Sci 1992;27:4678-84.
[68] Duncan O, Clegg F, Essa A, Bell AMT, Foster L, Allen T, et al. Effects of heat exposure and volumetric compression on Poisson's ratios, Young's moduli, and polymeric composition during thermo-mechanical conversion of auxetic open cell polyurethane foam. Phys Status Solidi B 2019;256:1800393.
[69] Bianchi M, Scarpa FL, Smith CW. Stiffness and energy dissipation in polyurethane auxetic foams. J Mater Sci 2008;43:5851-60.
[70] Critchley R, Smy V, Corni I, Wharton JA, Walsh FC, Wood RJK, et al. Experimental and computation assessment of thermomechanical effects during auxetic foam fabrication. Sci Rep 2020;10:18301.
[71] Lowe A, Lakes RS. Negative Poisson's ratio foam as seat cushion material. Cell Polym. 2000;19:157-67.
[72] Duncan O, Allen T, Foster L, Gatt R, Grima JN, Alderson A. Controlling density and modulus in auxetic foam fabrications - implications for impact and indentation testing. Proceedings 2018;2:250.
[73] Chaithanya Vinay V, Mohan Varma DS. Fabrication and testing of auxetic foams for rehabilitation applications. J Indian Inst Sci 2019;99:511-8.
[74] Khaderi SN, Kumar N, Rao KT. Impact on auxetic and metal foams. Vibroeng Proc 2019;29:255-9.
[75] Wei G. Negative and conventional Poisson’s ratios of polymeric networks with special microstructures. J Chem Phys 1992;96:3226-33.
[76] Warren WE, Kraynik AM. Foam mechanics - the Linear elastic response of two-dimensional spatially periodic cellular materials. Mech Mater 1987;6:27-37.
[77] Choi JB, Lakes RS. Nonlinear analysis of the Poisson's ratio of negative Poisson's ratio foams. J Compos Mater 2016;29:113-28.
[78] Doyoyo M, Wanhu J. Plastic failure analysis of an auxetic foam or inverted strut lattice under longitudinal and shear loads. J Mech Phys Solids 2006;54:1479-92.

[79] Chan N, Evans KE. Microscopic examination of themicrostructure and deformation of conventional and auxetic foams. J Mater Sci 1997;32:5725-36.
[80] Scarpa F, Yates JR, Ciffo LG, Patsias S. Dynamic crushing of auxetic open-cell polyurethane foam. Proc Inst Mech Eng Part C-J Eng Mech Eng Sci 2002;216:1153-6.
[81] Alderson A. A triumph of lateral thought. Chem Ind 1999:384-91.
[82] Alderson A, Rasburn J, Evans KE, Grima JN. Auxetic polymeric filters display enhanced de-fouling and pressure compensation properties. J Membr Sci Technol 2001;2001:6-8.
[83] Chan N, Evans KE. The mechanical properties of conventional and auxetic foams. Part II: Shear. J Cell Plast 2016;35:166-83.
[84] Gaspar N, Ren X, Smith C, Grima J, Evans K. Novel honeycombs with auxetic behaviour. Acta Mater 2005;53:2439-45.
[85] Lim TC, Alderson A, Alderson KL. Experimental studies on the impact properties of auxetic materials. Phys Status Solidi B 2014;251:307-13.
[86] Gaspar N, Smith CW, Miller EA, Seidler GT, Evans KE. Quantitative analysis of the microscale of auxetic foams. Phys Status Solidi B 2005;242:550-60.
[87] Grima JN, Evans KE. Auxetic behavior from rotating triangles. J Mater Sci 2006;41:3193-6.
[88] Grima JN, Chetcuti E, Manicaro E, Attard D, Camilleri M, Gatt R, et al. On the auxetic properties of generic rotating rigid triangles. Proc R Soc A-Math Phys Eng Sci 2011;468:810-30.
[89] Chetcuti E, Ellul B, Manicaro E, Brincat J-P, Attard D, Gatt R, et al. Modeling auxetic foams through semi-rigid rotating triangles. Phys Status Solidi B 2014;251:297-306.
[90] Pozniak AA, Smardzewski J, Wojciechowski KW. Computer simulations of auxetic foams in two dimensions. Smart Mater Struct 2013;22:084009.
[91] Li D, Dong L, Yin JH, Lakes RS. Negative Poisson's ratio in 2D Voronoi cellular solids by biaxial compression: a numerical study. J Mater Sci 2016;51:7029-37.
[92] Alderson A, Alderson KL, Davies P, Smart G. The effects of processing on the topology and mechanical properties of negative Poisson's ratio foams. Int Mech Eng Congress Expo 2005.
[93] McDonald SA, Dedreuil-Monet G, Yao YT, Alderson A, Withers PJ. In situ 3D X-ray microtomography study comparing auxetic and non-auxetic polymeric foams under tension. Phys Status Solidi B 2011;248:45-51.
[94] McDonald SA, Ravirala N, Withers PJ, Alderson A. In situ three-dimensional X-ray microtomography of an auxetic foam under tension. Scr Mater 2009;60:232-5.
[95] Elliott JA, Windle AH, Hobdell JR, Eeckhaut G, Oldman RJ, Ludwig W, et al. In-situ deformation of an open-cell flexible polyurethane foam characterised by 3D computed microtomography. J Mater Sci 2002;37:1547-55.
[96] Li Y, Zeng C. On the successful fabrication of auxetic polyurethane foams: Materials requirement, processing strategy and conversion mechanism. Polymer 2016;87:98-107.
[97] Pierron F, McDonald SA, Hollis D, Fu J, Withers PJ, Alderson A. Comparison of the mechanical behaviour of standard and auxetic foams by X-ray computed tomography and digital volume correlation. Strain 2013;49:467-82.
[98] Pierron F. Identification of Poisson's ratios of standard and auxetic low-density polymeric foams from full-field measurements. J Strain Anal Eng Des 2010;45:233-53.
[99] Lisiecki J, Kłysz S, Błażejewicz T, Gmurczyk G, Reymer P. Tomographic examination of auxetic polyurethane foam structures. Phys Status Solidi B 2014;251:314-20.
[100] Pashine N, Hexner D, Liu AJ, Nagel SR. Directed aging, memory, and nature's greed. Sci Adv 2019;5:eaax4215.
[101] Lv W, Li D, Dong L. Study on blast resistance of a composite sandwich panel with isotropic foam core with negative Poisson's ratio. Int J Mech Sci 2021;191.
[102] Mikulich Olena SL, Povstiana Yulia. Dynamic stress state of auxetic foam medium under the action of impulse load. Advances in Design, Simulation and Manufacturing II 2020. p. 623-32.
[103] Mott PH, Roland CM. Limits to Poisson’s ratio in isotropic materials. Phys Rev B 2009;80:132104.
[104] Gaspar N. Estimates for the localised stiffness and heterogeneity of auxetic foams. Phys Status Solidi B 2008;245:497-501.
[105] Mott PH, Roland CM. Limits to Poisson's ratio in isotropic materials - general result for arbitrary deformation. Phys Scr 2013;87:055404.
[106] Roh JH, Giller CB, Mott PH, Roland CM. Failure of classical elasticity in auxetic foams. AIP Adv 2013;3:042126.
[107] Roland CM, Mott PH, Calvo DC, Walker CN, Guild MD. Deviation from classical elasticity in the acoustic response of auxetic foams. Rubber Chem Technol 2017;90:381-6.
[108] Lakes RS. Design considerations for materials with negative Poisson’s ratios. J Mater Sci

1993;115:696-700.
[109] Choi J, Lakes R. Design of a fastener based on negative Poisson's ratio foam. Cell Polym 1991;10:205-12.
[110] Novak N, Duncan O, Allen T, Alderson A, Vesenjak M, Ren Z. Shear modulus of conventional and auxetic open-cell foam. Mech Mater. 2021;157:103818.
[111] Cheng HC, Scarpa F, Panzera TH, Farrow I, Peng H-X. Shear stiffness and energy absorption of auxetic open cell foams as sandwich cores. Phys Status Solidi B 2019;256:1800411
[112] Bianchi M, Scarpa F. Vibration transmissibility and damping behaviour for auxetic and conventional foams under linear and nonlinear regimes. Smart Mater Struct 2013;22:084010.
[113] Scarpa F, Ciffo LG, Yates JR. Dynamic properties of high structural integrity auxetic open cell foam. Smart Mater Struct 2004;13:49-56.
[114] Scarpa F, Bullough WA, Lumley P. Trends in acoustic properties of iron particle seeded auxetic polyurethane foam. Proc Inst Mech Eng Part C-J Eng Mech Eng Sci 2005;218:241-4.
[115] Scarpa F, Smith FC. Passive and MR fluid-coated auxetic PU foam - mechanical, acoustic, and electromagnetic properties. J Intell Mater Syst Struct 2016;15:973-9.
[116] Chekkal I, Bianchi M, Remillat C, Bécot FX, Jaouen L, Scarpa F. Vibro-acousticproperties of auxetic open cell foam: Model and experimental results. Acta Acust United Acust 2010;96:266-74.
[117] Hwan OJ, Seok KJ, Hiep NV, Kwon OI. Auxetic graphene oxide-porous foam for acoustic wave and shock energy dissipation. Compos B Eng 2020;186:107817.
[118] Gravade M OM, Collet M, Scarpa F, Bianchi M, Ichchou M. Auxetic transverse isotropic foams: from experimental efficiency to model correlation. Proceedings of the Acoustics. Nantes 2012.
[119] Alderson A, Rasburn J, Evans KE. Mass transport properties of auxetic (negative Poisson's ratio) foams. Phys Status Solidi B 2007;244:817-27.
[120] Gatt R, Attard D, Manicaro E, Chetcuti E, Grima JN. On the effect of heat and solvent exposure on the microstructure properties of auxetic foams: A preliminary study. Phys Status Solidi B. 2011;248:39-44.
[121] Yao Y, Luo Y, Xu Y, Wang B, Li J, Deng H, et al. Fabrication and characterization of auxetic shape memory composite foams. Compos B Eng 2018;152:1-7.
[122] N. Chan KEE. identation resilience of conventional and auxetic foams. J Cell Plast 1998;34:231-60.
[123] Bhullar SK. Characterization of auxetic polyurethanes foam for biomedical implants. e-Polymers 2014;14:441-7.
[124] Li D, Gao R, Dong L, Lam W-K, Zhang F. A novel 3D re-entrant unit cell structure with negative Poisson’s ratio and tunable stiffness. Smart Mater Struct 2020;29.
[125] Pastorino P, Scarpa F, Patsias S, Yates JR, Haake SJ, Ruzzene M. Strain rate dependence of stiffness and Poisson's ratio of auxetic open cell PU foams. Phys Status Solidi B 2007;244:955-65.
[126] Dirrenberger J, Forest S, Jeulin D. Effective elastic properties of auxetic microstructures: anisotropy and structural applications. Int J Mech Mater Des 2012;9:21-33.
[127] Grima JN, Ravirala N, Galea R, Ellul B, Attard D, Gatt R, et al. Modelling and testing of a foldable macrostructure exhibiting auxetic behaviour. Phys Status Solidi B 2011;248:117-22.
[128] Yang S, Qi C, Wang D, Gao R, Hu H, Shu J. A comparative study of ballistic resistance of sandwich panels with aluminum foam and auxetic honeycomb cores. Adv Mech Eng 2015;5:589216.
[129] Scarpa F, Pastorino P, Garelli A, Patsias S, Ruzzene M. Auxetic compliant flexible PU foams: static and dynamic properties. Phys Status Solidi B 2005;242:681-94.
[130] Lakes RS, Elms K. Indentability of conventional and negative Poisson's ratio foams. J Compos Mater 2016;27:1193-202.
[131] Bezazi A, Scarpa F. Tensile fatigue of conventional and negative Poisson’s ratio open cell PU foams. Int J Fatigue 2009;31:488-94.
[132] Sanami M, Ravirala N, Alderson K, Alderson A. Auxetic materials for sports applications. Procedia Eng 2014;72:453-8.
[133] Kumar N, Khaderi SN, Tirumala Rao K. Elasto-plastic indentation of auxetic and metal foams. J Appl Mech 2020;87:011006.
[134] Więcek T, Wasilewski A. Stiffness of auxetic foams. Acta Phys Pol A 2017;132:182-4.
[135] Li D, Dong L, Lakes RS. A unit cell structure with tunable Poisson's ratio from positive to negative. Mater Lett 2016;164:456-9.
[136] Wang YC, Lakes R. Analytical parametric analysis of the contact problem of human buttocks and negative Poisson's ratio foam cushions. Int J Solids Struct 2002;39:4825-38.
[137] Allen T, Shepherd J, Hewage TAM, Senior T, Foster L, Alderson A. Low-kinetic energy impact response of auxetic and conventional open-cell polyurethane foams. Phys Status Solidi B 2015;252:1631-9.
[138] Duncan O, Foster L, Senior T, Alderson A, Allen T. Quasi-static characterisation and impact testing of

auxetic foam for sports safety applications. Smart Mater Struct 2016;25:054014.
[139] Mohsenizadeh S, Alipour R, Shokri Rad M, Farokhi Nejad A, Ahmad Z. Crashworthiness assessment of auxetic foam-filled tube under quasi-static axial loading. Mater Des 2015;88:258-68.
[140] Mohsenizadeh S, Ahmad Z. Auxeticity effect on crushing characteristics of auxetic foam-filled square tubes under axial loading. Thin-Walled Struct 2019;145:106379.
[141] Mohsenizadeh S, Ahmad Z, Alias A. Numerical prediction on the crashworthiness of circular and square thin-walled tubes with polymeric auxetic foam core. J Mater Eng Perform 2020;29:3092-106.
[142] Yin H, Wen G, Liu Z, Qing Q. Crashworthiness optimization design for foam-filled multi-cell thin-walled structures. Thin-Walled Struct 2014;75:8-17.
[143] Zarei HR, Kröger M. Crashworthiness optimization of empty and filled aluminum crash boxes. Int J Crashworthiness 2007;12:255-64.
[144] F. Scarpa JG, Y. Zhang, P. Pastorino. Mechanical performance of auxetic polyurethane foam for antivibration glove applications. Cell Polym 2005;24: 253-68.
[145] Allen T, Duncan O, Foster L, Senior T, Zampieri D, Edeh V, et al. Auxetic foam for snow-sport safety devices. Snow Sports Trauma and Safety 2017. p. 145-59.
[146] Hou S, Liu T, Zhang Z, Han X, Li Q. How does negative Poisson’s ratio of foam filler affect crashworthiness? Mater Des 2015;82:247-59.
[147] Li D, Yin J, Dong L, Lakes RS. Strong re-entrant cellular structures with negative Poisson’s ratio. J Mater Sci 2017;53:3493-9.
[148] Lv W, Li D, Dong L. Study on mechanical properties of a hierarchical octet-truss structure. Compos Struct 2020;249.
[149] Bezazi A, Scarpa F. Mechanical behaviour of conventional and negative Poisson’s ratio thermoplastic polyurethane foams under compressive cyclic loading. Int J Fatigue 2007;29:922-30.
[150] Mohanraj H, Filho Ribeiro SLM, Panzera TH, Scarpa F, Farrow IR, Jones R, et al. Hybrid auxetic foam and perforated plate composites for human body support. Phys Status Solidi B 2016;253:1378-86.
[151] Foster L, Peketi P, Allen T, Senior T, Duncan O, Alderson A. Application of auxetic foam in sports helmets. Appl Sci 2018;8:354.
[152] Mohsenizadeh S, Alipour R, Nejad AF, Rad MS, Ahmad Z. Experimental investigation on energy absorption of auxetic foam-filled thin-walled square tubes under quasi-static loading. Procedia Manuf 2015;2:331-6.
[153] Zhang XY, Wang XY, Ren X, Xie YM, Wu Y, Zhou YY, et al. A novel type of tubular structure with auxeticity both in radial direction and wall thickness. Thin-Walled Struct 2021;163:107758.
[154] Zhanga XY, Ren X, Wang XY, Zhang Y, Xie YM. A novel combined auxetic tubular structure with enhanced tunable stiffness. Compos B Eng 2021.
[155] Strek T, Michalski J, Jopek H. Computational analysis of the mechanical impedance of the sandwich beam with auxetic metal foam core. Phys Status Solidi B 2019;256:1800423.
[156] Zahra T, Dhanasekar M. Characterisation of cementitious polymer mortar - Auxetic foam composites. Constr Build Mater 2017;147:143-59.
[157] Huang TT, Ren X, Zeng Y, Zhang Y, Luo C, Zhang XY, et al. Based on auxetic foam: A novel type of seismic metamaterial for Lamb waves. Eng Struct 2021;246.
[158] Lim TC. Torsion of semi-auxetic rods. J Mater Sci 2011;46:6904-9.
[159] Lim TC. Auxeticity of concentric auxetic-conventional foam rods with high modulus interface adhesive. Materials (Basel) 2018;11:223.
[160] Alderson A, Rasburn J, Ameer-Beg S, Mullarkey PG, Perrie W, Evans KE. An auxetic filter: A tuneable filter displaying enhanced size selectivity or defouling properties. Ind Eng Chem Res 2000;39:654-65.
[161] Bullogh WA, Scarpa F. Electrically controlled extension effects in soft solids. Int J Mod Phys B 2005;19:1655-60.
[162] Scarpa F, Bullough WA, Ruzzene M. Acoustic properties of auxetic foams with MR fluids. Noise Control and Acoustics 2003. p. 189-96.
[163] Alderson A, Alderson KL, McDonald SA, Mottershead B, Nazare S, Withers PJ, et al. Piezomorphic materials. Macromol Mater Eng 2013;298:318-27.
[164] Zhang SL, Lai Y-C, He X, Liu R, Zi Y, Wang ZL. Auxetic foam-based contact-mode triboelectric nanogenerator with highly sensitive self-powered strain sensing capabilities to monitor human body movement. Adv Funct Mater 2017;27:1606695.
[165] Ahmed MF, Li Y, Zeng C. Stretchable and compressible piezoresistive sensors from auxetic foam and silver nanowire. Mater Chem Phys 2019;229:167-73.
[166] La Malfa F, Puce S, Rizzi F, De Vittorio M. A flexible carbon nanotubes-based auxetic sponge electrode

for strain sensors. Nanomaterials (Basel) 2020;10:2365.
[167] Qi HJ, Boyce MC. Stress–strain behavior of thermoplastic polyurethanes. Mech Mater 2005;37:817-39.
[168] Somarathna HMCC, Raman SN, Mohotti D, Mutalib AA, Badri KH. Hyper-viscoelastic constitutive models for predicting the material behavior of polyurethane under varying strain rates and uniaxial tensile loading. Constr Build Mater 2020;236:117417.
[169] Lu W, Qin F, Wang Y, Luo Y, Wang H, Scarpa F, et al. Engineering graphene wrinkles for large enhancement of interlaminar friction enabled damping capability. ACS Appl Mater Interfaces 2019;11:30278-89.
[170] Jacobs LJM, Danen KCH, Kemmere MF, Keurentjes JTF. Quantitative morphology analysis of polymers foamed with supercritical carbon dioxide using Voronoi diagrams. Comput Mater Sci 2007;38:751-8.
[171] Bouakba M, Bezazi A, Scarpa F. FE analysis of the in-plane mechanical properties of a novel Voronoi-type lattice with positive and negative Poisson’s ratio configurations. Int J Solids Struct 2012;49:2450-9.
[172] L.Mu. Thiessen polygon. International Encyclopedia of Human Geography 2009:231-6.
[173] Yamada I. Thiessen polygons. International Encyclopedia of Geography: People, the Earth, Environment and Technology 2016. p. 1-6.
[174] Cosserat E, Cosserat F. Théorie des corps déformables 1909.
[175] Lakes RS. Experimental microelasticity of two porous solids. Int J Solids Struct 1986;22:55-63.
[176] Burns S. Negative Poisson's ratio materials. Science 1987;238:551.
[177] Ciambella J, Saccomandi G. A continuum hyperelastic model for auxetic materials. Proc R Soc A-Math Phys Eng Sci 2014;470:20130691.
[178] Gaspar N, Smith C, Evans K. Auxetic behaviour and anisotropic heterogeneity. Acta Mater 2009;57:875-80.
[179] Koenders MA. Constitutive properties of contacting materials with a finite-sized microstructure. Mol Simul 2005;31:873-82.
[180] Ciambella J, Bezazi A, Saccomandi G, Scarpa F. Nonlinear elasticity of auxetic open cell foams modeled as continuum solids. J Appl Phys 2015;117:184902.
[181] Rueger Z, Lakes RS. Cosserat elasticity of negative Poisson’s ratio foam: experiment. Smart Mater Struct 2016;25:054004.
[182] Amores VJ, San Millán FJ, Ben-Yelun I, Montáns FJ. A finite strain non-parametric hyperelastic extension of the classical phenomenological theory for orthotropic compressible composites. Compos B Eng 2021;212.
[183] Crespo J, Duncan O, Alderson A, Montáns FJ. Auxetic orthotropic materials: Numerical determination of a phenomenological spline-based stored density energy and its implementation for finite element analysis. Comput Methods Appl Mech Eng 2020;371.
[184] Ren X, Shen J, Tran P, Ngo TD, Xie YM. Auxetic nail: Design and experimental study. Compos Struct 2018;184:288-98.
[185] Ahmad, Zaini, Mohsenizadeh, Saeid, Alias, Amran, Alipour, Roozbeh. Influence of auxetic foam in quasi-static axial crushing. Int J Mater Res 2016;107:916-24.
[186] Fei Y, Chen F, Fang W, Xu L, Ruan S, Liu X, et al. High-strength, flexible and cycling-stable piezo-resistive polymeric foams derived from thermoplastic polyurethane and multi-wall carbon nanotubes. Compos B Eng 2020;199.
[187] Zhao J, Wang G, Chen Z, Huang Y, Wang C, Zhang A, et al. Microcellular injection molded outstanding oleophilic and sound-insulating PP/PTFE nanocomposite foam. Compos B Eng 2021;215.
[188] Zhu S, Zhou Q, Wang M, Dale J, Qiang Z, Fan Y, et al. Modulating electromagnetic interference shielding performance of ultra-lightweight composite foams through shape memory function. Compos B Eng 2021;204.
[189] Meng D, Liu X, Wang S, Sun J, Li H, Wang Z, et al. Self-healing polyelectrolyte complex coating for flame retardant flexible polyurethane foam with enhanced mechanical property. Compos B Eng 2021;219.
[190] Li T-T, Dai W, Huang S-Y, Wang H, Lin Q, Lin J-H, et al. Spring-like sandwich foam composites reinforced by 3D Concave–Convex structured fabric: Manufacturing and low-velocity cushion response. Compos B Eng 2020;197.
[191] Guo K-Y, Wu Q, Mao M, Chen H, Zhang G-D, Zhao L, et al. Water-based hybrid coatings toward mechanically flexible, super-hydrophobic and flame-retardant polyurethane foam nanocomposites with high-efficiency and reliable fire alarm response. Compos B Eng 2020;193.
[192] Wang L, Wu Y, Li Z, Jiang N, Niu K. Wavy graphene foam reinforced elastomeric composites for

large-strain stretchable conductors. Compos B Eng 2021;224.
[193] Carosio F, Negrell-Guirao C, Alongi J, David G, Camino G. All-polymer Layer by Layer coating as efficient solution to polyurethane foam flame retardancy. Eur Polym J 2015;70:94-103.
[194] Pan H, Lu Y, Song L, Zhang X, Hu Y. Construction of layer-by-layer coating based on graphene oxide/β-FeOOH nanorods and its synergistic effect on improving flame retardancy of flexible polyurethane foam. Compos Sci Techno 2016;129:116-22.
[195] Airoldi A, Novak N, Sgobba F, Gilardelli A, Borovinšek M. Foam-filled energy absorbers with auxetic behaviour for localized impacts. J Mater Sci Eng A 2020;788:139500.
[196] Yu R, Luo W, Yuan H, Liu J, He W, Yu Z. Experimental and numerical research on foam filled re-entrant cellular structure with negative Poisson's ratio. Thin-Walled Struct 2020;153:106679.
[197] Novak N, Krstulović-Opara L, Ren Z, Vesenjak M. Mechanical properties of hybrid metamaterial with auxetic chiral cellular structure and silicon filler. Compos Struct 2020;234:111718.